

Count Time Series Modeling with Gaussian Copulas ^{*†‡}

Yisu Jia Stefanos Kechagias
 University of North Florida SAS Institute
 James Livsey Robert Lund
 United States Census Bureau Clemson University
 Vladas Pipiras
 University of North Carolina

December 15, 2024

Abstract

This paper develops the theory and methods for copula modeling of a stationary count time series. The techniques use a latent Gaussian process and a distributional transformation to construct stationary series with very flexible correlation features that can have any pre-specified marginal distribution, including the classical Poisson, generalized Poisson, negative binomial, and binomial structures. A Gaussian pseudo-likelihood estimation paradigm, based only on the mean and autocovariance function of the count series, is developed via a new Hermite expansion. Particle filtering methods are used to conduct likelihood estimation. Connections to hidden Markov models are made. The performance of the estimation approaches are evaluated in a simulation study and the methods are used to analyze a count series of weekly retail sales.

1 Introduction

This paper develops the theory and methods for Gaussian copula modeling of stationary discrete-valued time series. Since the majority of discrete cases involve integer counts supported on some subset of $\{0, 1, \dots\}$, we hereafter isolate on this support set. Our methods are based on a copula transformation of a latent Gaussian stationary series and are able to produce any desired count marginal distribution. It is shown that the model class produces the most flexible pairwise correlation structures possible, including negatively dependent series.

^{*}AMS subject classification. Primary: 62M10. Secondary: 62J12, 62M05.

[†]Keywords and phrases: Count Data; Count Distributions; Generalized Poisson Distribution; Hermite Expansions; Hidden Markov Model; Likelihood Estimation; Negative Binomial Distribution; Time Series

[‡]Robert Lund's research was partially supported by the grant NSF DMS 1407480. Vladas Pipiras's research was partially supported by the grant NSF DMS 1712966.

Model parameters are estimated via 1) a Gaussian pseudo-likelihood approach, developed from some new Hermite expansion techniques, which use only the mean and the autocovariance of the series, 2) an implied Yule-Walker moment estimation approach in the case where the latent Gaussian process is an autoregression, and 3) a particle filtering approach that adapts hidden Markov model (HMM) techniques to general (not necessarily Markov) processes to approximate the true likelihood. Extensions to non-stationary settings, particularly those with covariates, are also discussed.

The theory of stationary Gaussian time series is by now well developed. A central result is that one can have a stationary Gaussian series $\{X_t\}_{t \in \mathbb{Z}}$, with lag- h autocovariance $\gamma_X(h) = \text{Cov}(X_t, X_{t+h})$, if and only if γ_X is symmetric ($\gamma_X(-h) = \gamma_X(h)$ for $h \in \mathbb{Z}^+$) and non-negative definite, viz.

$$\sum_{i=1}^k \sum_{j=1}^k a_i \gamma_X(t_i - t_j) a_j \geq 0$$

for every $k \in \{1, 2, \dots\}$, $t_i \in \mathbb{Z}$ and real numbers a_1, \dots, a_k (see Theorem 1.5.1 in [6]). Such a result does not hold for stationary count series. For example, existence of a stationary series with a Poisson marginal distribution is not guaranteed when γ_X is merely symmetric and non-negative definite. In fact, in the Poisson case, such a result is false: $\gamma_X(h) = (-1)^h$ is symmetric and non-negative definite, but it is impossible to have X_1 and X_2 jointly distributed with the same Poisson marginal distribution and a correlation of -1 (the reader is challenged to verify this). In principle, distributional existence issues are checked with Kolmogorov's consistency criterion (see Theorem 1.2.1 in [6]); in practice, one needs a specified joint distribution to check for consistency. Phrased another way, Kolmogorov's consistency criterion is not a constructive result and does not illuminate how to build stationary time series having a particular marginal distribution and correlation structure. Perhaps owing to this, count time series have been constructed from a plethora of approaches over the years. We now discuss some past approaches; a recent overview of stationary series is contained in [38]. While extensions to non-stationary cases with covariates are considered later, the fundamental problem lies with constructing stationary models.

Borrowing from the success of autoregressive moving-average (ARMA) models in describing stationary Gaussian series, early count authors constructed correlated count series from discrete autoregressive moving-average (DARMA) and integer autoregressive moving-average (INARMA) difference equation methods. Focusing on the first order autoregressive case for simplicity, a DAR(1) series $\{X_t\}_{t=1}^T$ with specified marginal distribution $F_X(\cdot)$ is obtained by generating X_1 from $F_X(\cdot)$ and then recursively setting

$$X_t = B_t X_{t-1} + (1 - B_t) Y_t, \quad t \in \{2, \dots, T\},$$

where $\{Y_t\}_{t=2}^T$ is generated as independent and identically distributed (IID) with marginal distribution $F_X(\cdot)$ and $\{B_t\}_{t=2}^T$ are generated IID independent Bernoulli trials, independent of $\{Y_t\}_{t=2}^T$, with $\mathbb{P}[B_t = 1] =: p \in (0, 1)$. Induction shows that X_t has marginal distribution $F_X(\cdot)$ for every t . INAR(1) series are built with a thinning operator \circ and parameter $p \in (0, 1)$ defined by $p \circ Y = \sum_{i=1}^Y B_i$ for any count valued random variable Y , where $\{B_i\}_{i=1}^\infty$ is again a collection of IID Bernoulli trials with success probability p . The INAR(1) difference equation is

$$X_t = p \circ X_{t-1} + \epsilon_t,$$

where $\{\epsilon_t\}$ is an IID count-valued random sequence.

DARMA methods were initially explored in [29, 30], but were subsequently discarded by practitioners because their sample paths often remain constant for long periods in highly correlated cases (observe that $\mathbb{P}[X_t = X_{t-1}] \geq p$ for DAR(1) series); INARMA series are still used today. Both INAR(1) and DAR(1) models have a correlation function of form $\text{Corr}(X_{t+h}, X_t) = p^h$, which cannot be negative since $p \in (0, 1)$. While one can add higher order autoregressive and even moving-average terms to the DAR(1) and INAR(1) setups (see [41, 42, 43]), all correlations remain non-negative. In contrast to their Gaussian ARMA brethren, DARMA and INARMA models do not span all possible correlation structures for stationary count series. Extensions of DARMA and INARMA methods are considered in [32], but none can produce negatively correlated series.

Blight [5] and [10] take a different approach, constructing the desired count marginal distribution by combining IID copies of a correlated Bernoulli series $\{B_t\}$ in various ways. By using a binary $\{B_t\}$ constructed from a stationary renewal sequence, a variety of marginal distributions, including binomial, Poisson, and negative binomial, were produced. While these models can have negative correlations [5, 10, 31], they do not necessarily produce the most negatively correlated count structures possible. The work in [37] derives explicit autocovariance functions when $\{B_t\}$ is made by binning (clipping) a stationary Gaussian sequence into zero-one categories and gives an example of a hurricane count data set where negative correlations arise. That said, some important count marginal distributions, including generalized Poisson, are not easily built from these methods. The results here easily generate any desired count marginal distribution.

Other count model classes studied include Gaussian based processes rounded to their nearest integer [34], hierarchical Bayesian count model approaches [3], generalized ARMA methods [4], and others. Each approach has some drawbacks. For example, rounding Gaussian processes to their nearest integer makes it difficult to produce a specific prescribed marginal distribution. Also, existing hierarchical Bayesian procedures typically posit conditional distributions in lieu of marginal distributions. For example, in a Poisson regression, the Poisson marginal stipulation is being imposed on the marginal distribution of the data. This is not the same as positing a conditional Poisson setup where one takes X_t given some random $\lambda_t > 0$ to have a Poisson distribution with mean λ_t . Indeed, as [2] shows, once the randomness of λ_t is taken into account, the true marginal distribution can be far from Poisson.

A time series analyst generally wants four features from a count model: 1) the ability to have a general marginal distribution; 2) the ability to have as general correlation structures as possible, both positive and negative; 3) the ability for the model to easily accommodate covariates; and 4) the ability to conduct likelihood inference. All previous count classes fail to accommodate one or more of these tenets. In fact, some count classes, like INARMA models, cannot achieve any of these features. This paper's purpose is to introduce and study a count model class that, for the first time, simultaneously allows all four features. Our model employs a latent Gaussian process and copula transformations. This type of construction has recently shown promise in spatial statistics [15, 25], multivariate modeling [47, 48], and regression [39], but the theory has yet to be developed for count series ([39, 36] provide some partial results). Our objectives here are several-fold. On a methodological level, it is shown, through some newly derived Hermite polynomial expansions, that accurate and

efficient numerical quantification of the correlation structure of the copula count model class is feasible. Based on a result of [51], the class is shown to produce the most flexible pairwise correlation structures possible (positive or negative) — see Remark 2.2 below. Connections to both importance sampling schemes, where the popular GHK sampler is adapted to our needs, and to the HMM literature, which allows natural extensions of the GHK sampler and likelihood evaluation, are made. All methods are tested on both synthetic and real data. Other prominent count time series works include [19, 13, 12, 20, 18].

The works [39, 36] are perhaps the closest papers to this study. While the general latent Gaussian construct adopted is the same, our work differs in that explicit autocovariance expansions are developed via Hermite expansions, flexibility and optimality issues of the model class are addressed, Gaussian pseudo-likelihood and implied least-squares parameter estimation are developed, and both the importance sampling and HMM connections are explored in detail. Additional connections to [39, 36] can be found in the main body of the paper. It is important to realize that our setting is the discrete case and that classical copula papers like [9] do not apply. The papers [25, 27] are also related and will be referenced below with commentary, but their focus is on spatial count modeling.

The rest of this paper proceeds as follows. The next section introduces our Gaussian copula count model and establishes its basic mathematical and statistical properties. Section 3 moves to estimation, developing three techniques. The first method, a Gaussian pseudo-likelihood approach involving only the mean and covariance of the series, can be numerically optimized to rapidly obtain model parameter estimates. The second method modifies Yule-Walker moment estimation to the case where the latent Gaussian process obeys an autoregressive structure. The third method uses particle filtering techniques to construct an approximation of the true likelihood of the series. Here, connections to HMM and importance sampling methodologies are made. Section 4 presents simulation results, showing a case where Gaussian pseudo-likelihood performs reasonably well, and a case where particle filtering likelihood estimates, which feel the entire joint count distributional structure, are superior. Section 5 analyzes sales count series of a soft drink sold at one location of the now defunct Dominick’s Finer Foods. The series exhibits overdispersion, negative lag one autocorrelation, and dependence on a price reduction (sales) covariate, illustrating the flexibility of our approach. Section 6 closes the paper with comments and suggestions for future research.

2 Theory

We are interested in constructing stationary time series $\{X_t\}$ having marginal distributions from several families of count structures supported in $\{0, 1, \dots\}$, including:

- Binomial (Bin(N, p)): $\mathbb{P}[X_t = k] = \binom{N}{k} p^k (1 - p)^{N-k}$, $k \in \{0, \dots, N\}$, $p \in (0, 1)$;
- Poisson (Pois(λ)): $\mathbb{P}[X_t = k] = e^{-\lambda} \lambda^k / k!$, with $\lambda > 0$;
- Mixture Poisson (mixPois($\boldsymbol{\lambda}, \mathbf{p}$)): $\mathbb{P}[X_t = k] = \sum_{m=1}^M p_m e^{-\lambda_m} \lambda_m^k / k!$, where $\mathbf{p} = (p_1, \dots, p_M)'$ with the mixture probabilities $p_m > 0$ such that $\sum_{m=1}^M p_m = 1$ and $\boldsymbol{\lambda} = (\lambda_1, \dots, \lambda_M)'$ with $\lambda_m > 0$ for each m ;

- Negative binomial (NB(r, p)): $\mathbb{P}[X_t = k] = \frac{\Gamma(r+k)}{k!\Gamma(r)}(1-p)^r p^k$, with $r > 0$ and $p \in (0, 1)$;
- Generalized Poisson (GPois(λ, η)): $\mathbb{P}[X_t = k] = e^{-(\lambda+\eta k)} \lambda(\lambda + \eta k)^{k-1}/k!$, with $\lambda > 0$ and $\eta \in [0, 1)$;
- Conway-Maxwell-Poisson (CMP(λ, ν)): $\mathbb{P}[X_t = k] = \frac{\lambda^k}{(k!)^\nu C(\lambda, \nu)}$, with $\lambda > 0$, $\nu > 0$, and a normalizing constant $C(\lambda, \nu)$ making the probabilities sum to unity.

The negative binomial, generalized Poisson, and Conway-Maxwell-Poisson distributions are over-dispersed in that their variances are larger than their respective means. This is the case for many observed count time series.

Let $\{X_t\}_{t \in \mathbb{Z}}$ be the stationary count time series of interest. Suppose that one wants the marginal cumulative distribution function (CDF) of X_t for each t of interest to be $F_X(x) = \mathbb{P}[X_t \leq x]$, depending on a vector $\boldsymbol{\theta}$ containing all CDF model parameters. The series $\{X_t\}$ will be modeled through

$$X_t = G(Z_t), \quad (1)$$

where

$$G(z) = F_X^{-1}(\Phi(z)), \quad z \in \mathbb{R}, \quad (2)$$

and $\Phi(\cdot)$ is the CDF of a standard normal variable and

$$F_X^{-1}(u) = \inf\{t : F_X(t) \geq u\}, \quad u \in (0, 1), \quad (3)$$

is the generalized inverse (quantile function) of the non-decreasing CDF F_X . The process $\{Z_t\}_{t \in \mathbb{Z}}$ is assumed to be standard Gaussian, but possibly correlated in time t :

$$\mathbb{E}[Z_t] = 0, \quad \mathbb{E}[Z_t^2] = 1, \quad \rho_Z(h) = \text{Corr}(Z_t, Z_{t+h}) = \mathbb{E}[Z_t Z_{t+h}]; \quad (4)$$

that is, $Z_t \sim \mathcal{N}(0, 1)$ for each t . This approach has been recently used by [47, 39, 25] with good results. The autocovariance function (ACVF) of $\{Z_t\}$, denoted by $\gamma_Z(\cdot)$, is the same as the autocorrelation function (ACF) due to the standard normal assumption and depends on another vector $\boldsymbol{\eta}$ of ACVF parameters.

The model in (1)–(3) has appeared in other bodies of literature under different nomenclature. In particular, [7, 8] call this setup the normal to anything (NORTA) procedure in operations research and [23] calls this a translational model in mechanical engineering. Our goal is to give a reasonably complete analysis of the probabilistic and statistical properties of these models.

The construction in (1) ensures that the marginal CDF of X_t is indeed $F_X(\cdot)$. Elaborating, the probability integral transformation theorem shows that $\Phi(Z_t)$ has a uniform distribution over $(0, 1)$ for each t ; a second application of the result justifies that X_t has marginal distribution $F_X(\cdot)$ for each t . Temporal dependence in $\{Z_t\}$ will induce temporal dependence in $\{X_t\}$ as quantified below. For notation, let

$$\gamma_X(h) = \mathbb{E}[X_{t+h} X_t] - \mathbb{E}[X_{t+h}] \mathbb{E}[X_t] \quad (5)$$

denote the ACVF of $\{X_t\}$.

2.1 Relationship between autocovariances

The autocovariance functions of $\{X_t\}$ and $\{Z_t\}$ can be related using Hermite expansions (see Chapter 5 of [46]). More specifically, let

$$G(z) = \mathbb{E}[G(Z_0)] + \sum_{k=1}^{\infty} g_k H_k(z) \quad (6)$$

be the expansion of $G(z)$ in terms of the Hermite polynomials

$$H_k(z) = (-1)^k e^{z^2/2} \frac{d^k}{dz^k} \left(e^{-z^2/2} \right), \quad z \in \mathbb{R}. \quad (7)$$

The first three Hermite polynomials are $H_0(z) \equiv 1$, $H_1(z) = z$, and $H_2(z) = z^2 - 1$; higher order polynomials can be obtained from the recursion $H_k(z) = zH_{k-1}(z) - H'_{k-1}(z)$. The *Hermite coefficients* are

$$g_k = \frac{1}{k!} \int_{-\infty}^{\infty} G(z) H_k(z) \frac{e^{-z^2/2} dz}{\sqrt{2\pi}} = \frac{1}{k!} \mathbb{E}[G(Z_0) H_k(Z_0)]. \quad (8)$$

The relationship between $\gamma_X(\cdot)$ and $\gamma_Z(\cdot)$ is key and is extracted from Chapter 5 of [46] as

$$\gamma_X(h) = \sum_{k=1}^{\infty} k! g_k^2 \gamma_Z(h)^k =: g(\gamma_Z(h)), \quad (9)$$

where the power series is

$$g(u) = \sum_{k=1}^{\infty} k! g_k^2 u^k. \quad (10)$$

In particular,

$$\text{Var}(X_t) = \gamma_X(0) = \sum_{k=1}^{\infty} k! g_k^2 \quad (11)$$

depends only on the parameters in the marginal distribution F_X . Note also that

$$\rho_X(h) = \sum_{k=1}^{\infty} \frac{k! g_k^2}{\gamma_X(0)} \gamma_Z(h)^k =: L(\rho_Z(h)), \quad (12)$$

where

$$L(u) = \sum_{k=1}^{\infty} \frac{k! g_k^2}{\gamma_X(0)} u^k =: \sum_{k=1}^{\infty} \ell_k u^k \quad (13)$$

and $\ell_k = k! g_k^2 / \gamma_X(0)$. The function L maps $[-1, 1]$ into (but not necessarily onto) $[-1, 1]$. An error bound when the sum in (13) is truncated to M terms is derived in [25]. For future reference, note that $L(0) = 0$ and by (11),

$$L(1) = \sum_{k=1}^{\infty} \ell_k = 1. \quad (14)$$

Using (6) and $\mathbb{E}[H_k(Z_0)H_\ell(-Z_0)] = (-1)^k k! 1_{[k=\ell]}$ gives

$$L(-1) = \text{Corr}(G(Z_0), G(-Z_0)); \quad (15)$$

however, $L(-1)$ is not necessarily -1 in general. As such, $L(\cdot)$ “starts” at $(-1, L(-1))$, passes through $(0, 0)$, and connects to $(1, 1)$. Examples will be given in Section 2.4.

From (12), one can see that

$$|\rho_X(h)| \leq |\rho_Z(h)|. \quad (16)$$

This will be useful later. Equation (12) shows that a positive $\rho_Z(h)$ leads to a positive $\rho_X(h)$. A negative $\rho_Z(h)$ produces a negative $\rho_X(h)$ since $L(u)$ is, in fact, monotone increasing (see Proposition 2.1 below) and crosses zero at $u = 0$ (the negativeness of $\rho_X(h)$ when $\rho_Z(h) < 0$ can also be deduced from the nondecreasing nature of G via an inequality on page 20 of [50] for Gaussian variables).

The quantity $L(\cdot)$ is called a *link* function, and ℓ_k , $k \geq 1$, are called *link coefficients*. (Sometimes, slightly abusing the terminology, we also use these terms for $g(\cdot)$ and $g_k^2 k!$, respectively.) A key feature in (9) is that the effects of the marginal CDF $F_X(\cdot)$ and the ACVF $\gamma_Z(\cdot)$ are “decoupled” in the sense that the correlation parameters in $\{Z_t\}$ do not influence the g_k coefficients in (9) — this is useful in estimation later.

Remark 2.1. The short- and long-range dependence properties of $\{X_t\}$ can be extracted from those of $\{Z_t\}$. Recall that a time series $\{Z_t\}$ is short-range dependent (SRD) if $\sum_{h=-\infty}^{\infty} |\rho_Z(h)| < \infty$. According to one definition, a series $\{Z_t\}$ is long-range dependent (LRD) if $\rho_Z(h) = Q(h)h^{2d-1}$, where $d \in (0, 1/2)$ is the LRD parameter and Q is a slowly varying function at infinity [46]. The ACVF of such LRD series satisfies $\sum_{h=-\infty}^{\infty} |\rho_Z(h)| = \infty$. If $\{Z_t\}$ is SRD, then so is $\{X_t\}$ by (16). On the other hand, if $\{Z_t\}$ is LRD with parameter d , then $\{X_t\}$ can be either LRD or SRD. The conclusion depends, in part, on the Hermite rank of $G(\cdot)$, which is defined as $r = \min\{k \geq 1 : g_k \neq 0\}$. Specifically, if $d \in (0, (r-1)/2r)$, then $\{X_t\}$ is SRD; if $d \in ((r-1)/2r, 1/2)$, then $\{X_t\}$ is LRD with parameter $r(d-1/2)+1/2$ (see [46], Proposition 5.2.4). For example, when the Hermite rank is unity, $\{X_t\}$ is LRD with parameter d for all $d \in (0, 1/2)$; when $r = 2$, $\{X_t\}$ is LRD with parameter $2d - 1/2$ for $d \in (1/4, 1/2)$.

Remark 2.2. The construction in (1)–(2) yields models with very flexible autocorrelations. In fact, the methods achieve the most flexible correlation possible for $\text{Corr}(X_{t_1}, X_{t_2})$ when X_{t_1} and X_{t_2} have the same marginal distribution F_X . Indeed, let $\rho_- = \min\{\text{Corr}(X_{t_1}, X_{t_2}) : X_{t_1}, X_{t_2} \sim F_X\}$ and define ρ_+ similarly with min replaced by max. Then, as shown in Theorem 2.5 of [51],

$$\rho_+ = \text{Corr}(F_X^{-1}(U), F_X^{-1}(U)) = 1, \quad \rho_- = \text{Corr}(F_X^{-1}(U), F_X^{-1}(1-U)),$$

where U is a uniform random variable over $(0, 1)$. Since $U \stackrel{\mathcal{D}}{=} \Phi(Z)$ and $1-U \stackrel{\mathcal{D}}{=} \Phi(-Z)$ for a standard normal random variable Z , the maximum and minimum correlations ρ_+ and ρ_- are indeed achieved with (1)–(2) when $Z_{t_1} = Z_{t_2}$ and $Z_{t_1} = -Z_{t_2}$, respectively. The preceding statements are non-trivial for ρ_- only since $\rho_+ = 1$ is attained whenever $X_{t_1} = X_{t_2}$. It is worthwhile to compare this to the discussion surrounding (15). Finally, all correlations in $(\rho_-, \rho_+) = (\rho_-, 1)$ are achievable since $L(u)$ in (13) is continuous in u . The flexibility of correlations for Gaussian copula models in the spatial context was also noted and studied in [25], especially when compared to a competing class of hierarchical, e.g. Poisson, models.

The preceding remark all but settles flexibility of autocovariance debates for stationary count series. Flexibility is a concern when the count series is negatively correlated, an issue arising in the hurricane data in [37] and with chemical process data in [34]. Since a general count marginal distribution can also be achieved, the model class is quite general.

2.2 Covariates

There are situations where stationarity is not desired. Such scenarios can often be accommodated by simple variants of the above setup. For concreteness, consider a situation where J non-random covariates are available to explain the series at time t — call these $M_{1,t}, \dots, M_{J,t}$. If one wants X_t to have the marginal distribution $F_{\boldsymbol{\theta}(t)}(\cdot)$, where $\boldsymbol{\theta}(t)$ is a vector-valued function of t containing parameters, then simply set

$$X_t = F_{\boldsymbol{\theta}(t)}^{-1}(\Phi(Z_t)) \quad (17)$$

and reason as before. We do not recommend modifying $\{Z_t\}$ for the covariates as this may bring process existence issues into play.

Link functions, not to be confused with $L(\cdot)$ in (12)–(13), can be used when parametric support set bounds are encountered. As an example, a Poisson regression with correlated errors can be formulated via

$$\boldsymbol{\theta}(t) = \mathbb{E}[X_t] = \exp\left(\beta_0 + \sum_{j=1}^J \beta_j M_{j,t}\right).$$

Here, the exponential link guarantees that the Poisson parameter is positive and β_0, \dots, β_J are regression coefficients. The above construct requires the covariates to be non-random; should covariates be random, the marginal distribution may change.

2.3 Calculation and properties of the Hermite coefficients

Several strategies for Hermite coefficient computation are available. We consider the stationary setting here for simplicity. As $G(\cdot)$ in (2) is discrete, the following approach proved simple, numerically stable, and revealing. Recall that $\boldsymbol{\theta}$ denotes all parameters appearing in the marginal distribution F_X . For $\boldsymbol{\theta}$ fixed, define the mass and cumulative probabilities of F_X via

$$p_n = \mathbb{P}[X_t = n], \quad C_n = \mathbb{P}[X_t \leq n] = \sum_{j=0}^n p_j, \quad n \in \{0, 1, \dots\}, \quad (18)$$

where dependence on $\boldsymbol{\theta}$ is notationally suppressed. Note that

$$G(z) = \sum_{n=0}^{\infty} n \mathbb{1}_{\{C_{n-1} \leq \Phi(z) < C_n\}} = \sum_{n=0}^{\infty} n \mathbb{1}_{[\Phi^{-1}(C_{n-1}), \Phi^{-1}(C_n))}(z) \quad (19)$$

(take $C_{-1} = 0$ as a convention). When $C_n = 0$, we take $\Phi^{-1}(C_n) = -\infty$; when $C_n = 1$, we take $\Phi^{-1}(C_n) = \infty$. Using this in (8) provides, for $k \geq 1$,

$$g_k = \frac{1}{k!} \mathbb{E}[G(Z_0) H_k(Z_0)] = \frac{1}{k!} \sum_{n=0}^{\infty} n \mathbb{E}\left[\mathbb{1}_{[\Phi^{-1}(C_{n-1}), \Phi^{-1}(C_n))}(Z_0) H_k(Z_0)\right].$$

Plugging (7) into the above equation and simplifying provides

$$\begin{aligned}
g_k &= \frac{1}{k!} \sum_{n=0}^{\infty} \frac{n}{\sqrt{2\pi}} \int_{\Phi^{-1}(C_{n-1})}^{\Phi^{-1}(C_n)} H_k(z) e^{-z^2/2} dz \\
&= \frac{1}{k!} \sum_{n=0}^{\infty} \frac{n}{\sqrt{2\pi}} \int_{\Phi^{-1}(C_{n-1})}^{\Phi^{-1}(C_n)} (-1)^k \left(\frac{d^k}{dz^k} e^{-z^2/2} \right) dz \\
&= \frac{1}{k!} \sum_{n=0}^{\infty} \frac{n}{\sqrt{2\pi}} (-1)^k \left(\frac{d^{k-1}}{dz^{k-1}} e^{-z^2/2} \right) \Big|_{z=\Phi^{-1}(C_{n-1})}^{\Phi^{-1}(C_n)} \\
&= \frac{1}{k!} \sum_{n=0}^{\infty} \frac{n}{\sqrt{2\pi}} (-1) e^{-z^2/2} H_{k-1}(z) \Big|_{z=\Phi^{-1}(C_{n-1})}^{\Phi^{-1}(C_n)} \\
&= \frac{1}{k! \sqrt{2\pi}} \sum_{n=0}^{\infty} n \left[e^{-\Phi^{-1}(C_{n-1})^2/2} H_{k-1}(\Phi^{-1}(C_{n-1})) - e^{-\Phi^{-1}(C_n)^2/2} H_{k-1}(\Phi^{-1}(C_n)) \right]. \quad (20)
\end{aligned}$$

The telescoping nature of the series in (20) provides

$$g_k = \frac{1}{k! \sqrt{2\pi}} \sum_{n=0}^{\infty} e^{-\Phi^{-1}(C_n)^2/2} H_{k-1}(\Phi^{-1}(C_n)) \quad (21)$$

(convergence issues are addressed in Lemma 2.1 below). When $\Phi^{-1}(C_n) = \pm\infty$ (that is, $C_n = 0$ or 1), the summand $e^{-\Phi^{-1}(C_n)^2/2} H_{k-1}(\Phi^{-1}(C_n))$ is interpreted as zero. Before proceeding, the following results will clarify several coefficient issues. The key technical step is Lemma 2.1 below. As noted in these remarks and the next section, (21) is appealing from a numerical standpoint; it also sheds light on the behavior of the Hermite coefficients.

Lemma 2.1. *The representation in (21) is valid whenever $\mathbb{E}[X_t^p] < \infty$ for some $p > 1$.*

Proof. Observe that one obtains (21) from (20) if, after changing $k-1$ to k for notational simplicity,

$$\sum_{n=0}^{\infty} e^{-\Phi^{-1}(C_n)^2/2} \left| H_k(\Phi^{-1}(C_n)) \right| < \infty. \quad (22)$$

To see that this holds when $\mathbb{E}[X_t^p] < \infty$ for some $p > 1$, suppose that $C_n < 1$ for all n , since otherwise the sum in (22) has a finite number of terms. Since $H_k(z)$ is a polynomial of degree k , $|H_k(z)| \leq \kappa(1 + |z|^k)$ for some constant κ that depends on k . The sum in (22) can hence be bounded (up to a constant) by

$$\sum_{n=0}^{\infty} e^{-\Phi^{-1}(C_n)^2/2} (1 + |\Phi^{-1}(C_n)|^k). \quad (23)$$

To show that (23) converges, it suffices to show that

$$\sum_{n=0}^{\infty} e^{-\Phi^{-1}(C_n)^2/2} |\Phi^{-1}(C_n)|^k < \infty \quad (24)$$

since $|\Phi^{-1}(C_n)|^k \uparrow \infty$ as $C_n \uparrow 1$. Mill's ratio for a standard normal distribution states that $1 - \Phi(x) \sim e^{-x^2/2}/(\sqrt{2\pi}x)$ as $x \rightarrow \infty$. Substituting $x = \Phi^{-1}(y)$ gives $1 - y \sim e^{-\Phi^{-1}(y)^2/2}/(\sqrt{2\pi}\Phi^{-1}(y))$ as $y \uparrow 1$. Taking logarithms in the last relation and ignoring constant terms, order arguments show that $\Phi^{-1}(y) \sim \sqrt{2}|\log(1 - y)|^{1/2}$ as $y \uparrow 1$. Substituting $\Phi^{-1}(C_n) \sim \sqrt{2}|\log(1 - C_n)|^{1/2}$ into (24) provides

$$\sum_{n=0}^{\infty} e^{-\Phi^{-1}(C_n)^2/2} |\Phi^{-1}(C_n)|^k \leq \sum_{n=0}^{\infty} (1 - C_n) |\log(1 - C_n)|^{k/2}. \quad (25)$$

For any $\delta > 0$ and $x \in (0, 1)$, one can verify that $-\log(x) \leq x^{-\delta}/\delta$. Using this in (25) and $C_n = 1 - \mathbb{P}[X > n]$, it suffices to prove that

$$\sum_{n=0}^{\infty} \mathbb{P}[X > n]^{1-\delta k/2} < \infty \quad (26)$$

for some $\delta > 0$. Since $X \geq 0$ and $\mathbb{E}[X^p] < \infty$ are assumed, the Markov inequality gives $\mathbb{P}[X > n] = \mathbb{P}[X^p > n^p] \leq \mathbb{E}[X^p]/n^p$. Thus the sum in (26) is bounded by

$$\mathbb{E}[X^p]^{1-\delta k/2} \sum_{n=0}^{\infty} \frac{1}{n^{p-p\delta k/2}}. \quad (27)$$

But (27) converges whenever $\delta < 2(p-1)/(pk)$. Choosing such a δ proves (22) and finishes our work. \square

Remark 2.3. From a numerical standpoint, the expression in (21) is evaluated as follows. The families of marginal distributions considered in this work have fairly “light” tails, meaning that C_n approaches unity rapidly as $n \rightarrow \infty$. This means that C_n becomes *exactly unity numerically* for small to moderate values of n . Let $n(\boldsymbol{\theta})$ be the smallest such value. For example, for the Poisson distribution with parameter $\boldsymbol{\theta} = \lambda$ and Matlab software, $n(0.1) = 10$, $n(1) = 19$, and $n(10) = 47$. For $n \geq n(\boldsymbol{\theta})$, the numerical value of $\Phi^{-1}(C_n)$ is infinite and the terms $e^{-\Phi^{-1}(C_n)^2/2} H_{k-1}(\Phi^{-1}(C_n))$ in (21) are numerically zero and can be discarded. Thus, (21) becomes

$$g_k = \frac{1}{k! \sqrt{2\pi}} \sum_{n=0}^{n(\boldsymbol{\theta})-1} e^{-\Phi^{-1}(C_n)^2/2} H_{k-1}(\Phi^{-1}(C_n)). \quad (28)$$

Alternatively, one could calculate the Hermite coefficients using Gaussian quadrature methods, as discussed e.g. in [25], p. 51. The approach based on (28) though is certainly simpler numerically. Furthermore, as noted below, the expression (28) can shed further light on the behavior of the Hermite coefficients.

Remark 2.4. Assuming that the g_k are evaluated through (28), their asymptotic behavior as $k \rightarrow \infty$ can be quantified. We focus on $g_k(k!)^{1/2}$, whose squares are the link coefficients. The asymptotic relation for Hermite polynomials states that $H_m(x) \sim e^{x^2/4} (m/e)^{m/2} \sqrt{2} \cos(x\sqrt{m} - m\pi/2)$ as $m \rightarrow \infty$ for each $x \in \mathbb{R}$. Using this and Stirling's formula ($k! \sim k^k e^{-k} \sqrt{2\pi k}$ as $k \rightarrow \infty$) show that

$$g_k(k!)^{1/2} \sim \frac{1}{2^{1/4} \pi^{3/4}} \frac{1}{k^{3/4}} \sum_{n=0}^{n(\boldsymbol{\theta})-1} e^{-\Phi^{-1}(C_n)^2/4} \cos \left(\Phi^{-1}(C_n) \sqrt{k-1} - \frac{(k-1)\pi}{2} \right). \quad (29)$$

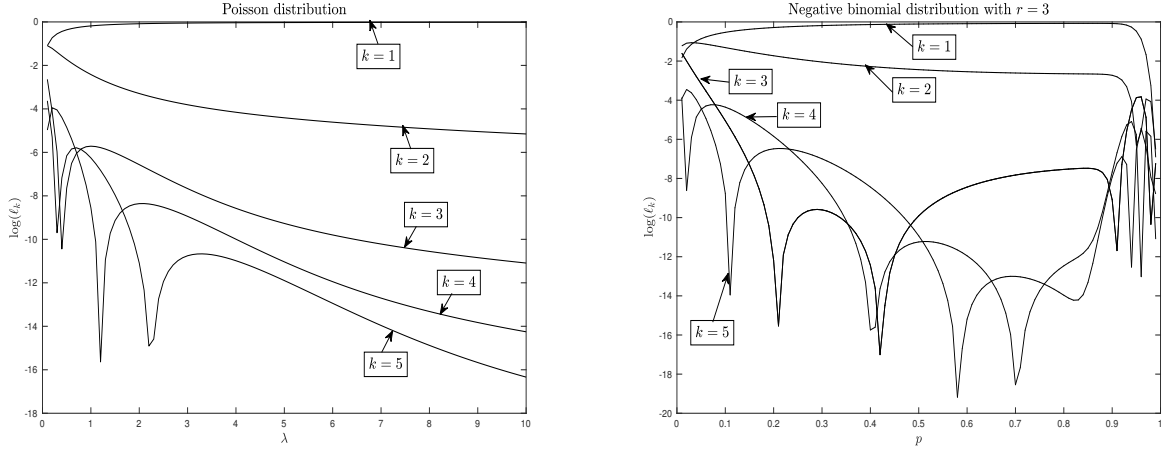


Figure 1: The link coefficients ℓ_k on a log-vertical scale for the Poisson (left) and negative binomial (right) distributions.

Numerically, this approximation, which does not involve Hermite polynomials, was found to be accurate for even moderate values of k . It implies that $k!g_k^2$ decays (up to a constant) as $k^{-3/2}$. While this might seem slow, these coefficients are multiplied by $\gamma_Z(h)^k = \rho_Z(h)^k$ in (9), which decay geometrically in k to zero, except in degenerate cases when $|\rho_Z(h)| = 1$.

The computation and behavior of the link coefficients ℓ_k are now examined for several families of marginal distributions. Figure 1 shows plots of ℓ_k on a vertical log scale over a range of parameter values for $k \in \{1, \dots, 5\}$ for the Poisson and negative binomial (with $r = 3$) distributions. A number of observations are worth making.

Since $\sum_{k=1}^{\infty} \ell_k = 1$ and $\ell_k \geq 0$ by construction, the parameter values in Figure 1 with $\log(\ell_1)$ close to 0 (or ℓ_1 close to 1) implies that most of the “weight” in the link coefficients is contained in the first coefficient, with higher order coefficients being considerably smaller and decaying with increasing k . This takes place in the approximate ranges $\lambda > 1$ for the Poisson distribution and $p \in (0.1, 0.9)$ in the negative binomial distribution with $r = 3$. Such cases will be called “condensed”. As shown in Section 2.4 below, $L(u)$ in the condensed case is close to u . In the condensed case, correlations in $\{Z_t\}$ and $\{X_t\}$ are similar.

Non-condensed cases are referred to as “diffuse”. Here, weight is spread to many link coefficients. This happens in the approximate ranges $\lambda < 1$ for the Poisson distribution and $p < 0.1$ and $p > 0.9$ for the negative binomial distribution with $r = 3$. This was expected for small λ s and small p s: these cases correspond to discrete random structures that are nearly degenerate in the sense that they concentrate at 0 (as $\lambda \rightarrow 0$ or $p \rightarrow 0$). For such cases, large negative correlations in (15) are not possible; hence, $L(u)$ cannot be close to u and correlations in $\{Z_t\}$ and $\{X_t\}$ are different. The diffuse range $p > 0.9$ for the negative binomial distribution remains to be understood, although it is likely again some form of degeneracy.

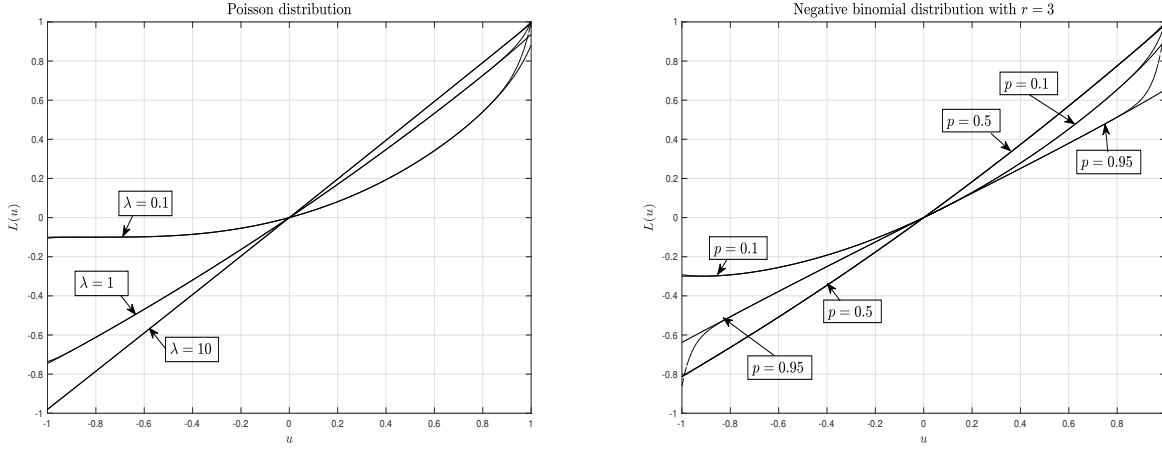


Figure 2: The link function L for the Poisson distribution with $\lambda = 0.1, 1$, and 10 (left) and the negative binomial distribution with $r = 3$ and $p = 0.1, 0.5$, and 0.95 (right).

2.4 Calculation and properties of link functions

We now study calculation of $L(u)$ in (13), which requires truncation of the sum to $k \in \{1, \dots, K\}$ for some K . Note again that the link coefficients ℓ_k are multiplied by $\gamma_Z(h)^k = \rho_Z(h)^k$ in (9) before they are summed, and the latter decays to zero geometrically rapidly in k for most stationary $\{Z_t\}$ when $h \neq 0$. The link coefficients for large k are therefore expected to play a minor role. We now set $K = 25$ and explore consequences of this choice.

Remark 2.5. An alternative procedure would bound (29) by $(2\pi^3 k^3)^{-1/4} \sum_{n=0}^{n(\theta)-1} e^{-\Phi^{-1}(C_n)^2/4}$. Now let $K = K(\theta)$ be the smallest k for which the bound is smaller than some preset error tolerance ϵ . In the Poisson case with $\epsilon = 0.01$, for example, such K are $K(0.01) = 29$, $K(0.1) = 27$, and $K(1) = 25$. These are close to the chosen value of $K = 25$. A different bound and resulting truncation in the spatial context can be found in [25], Lemma 2.2.

Figure 2 plots $L(u)$ (solid line) for the Poisson and negative binomial distributions for several parameter values. The link function is computed by truncating its expansion to $k \leq 25$ as discussed above. The condensed cases $\lambda = 10$ and $\lambda = 1$ (perhaps this case is less condensed) and $p = 0.85$ lead to curves with $L(u) \approx u$. However, the diffuse cases appear more delicate. Diffusivity and truncation of the infinite series in (13) lead to a computed link function that does not have $L(1) = 1$ (see (14)); in this case, one should increase the number of terms in the summation.

Though deviations from $L(1) = 1$ might seem large (most notably for the negative binomial distribution with $p = 0.95$), this seems to arise only in the more degenerate cases associated with diffusivity; moreover, this occurs only when linking an ACVF of $\{Z_t\}$ for lags h for which $\rho_Z(h)$ is close to unity. For example, note that if the link deviation is 0.2 from unity at $u = 1$ (as it is approximately for the negative binomial distribution with $p = 0.95$), the error for linking $\rho_Z(h)$ as 0.8 (or smaller but positive) would be no more than $0.2(0.8)^{26} \approx 0.0006$. In practice, any link deviation could be partially corrected by adding one extra ‘‘pseudo link coefficient’’, in our case, a 26th coefficient, which would make the link function pass through $(1, 1)$. The resulting link function is depicted in the dashed line

in Figure 2 around the point $(1, 1)$ and essentially coincides with the original link function for all u 's except possibly for u values that are close to unity.

The situation for negative u and, in particular, around $u = -1$ is different: the theoretical value of $L(-1)$ in (15) is not explicitly known. However, a similar correction could be achieved by first estimating $L(-1)$ through a Monte-Carlo simulation and adding a pseudo 26th coefficient making the computed link function connect to the desired value at $u = -1$. This is again depicted for negative u via the dashed lines in Figure 2, which is visually distinguishable only near $u = -1$ (and then only in some cases). Again, one cannot have a count process whose lag one correlation is more negative than $L(-1)$ — such a count series does not exist by Remark 2.2.

Remark 2.6. In our ensuing estimation work, a link function needs to be evaluated multiple times; hence, running Monte-Carlo simulations to evaluate $L(-1)$ can become computationally expensive. In this case, the estimation procedure is fed precomputed values of $L(-1)$ on a grid of parameter values and interpolation is used for intermediate parameter values.

The next result further quantifies the link function's structure. The result implies that $\rho_X(h)$ is nondecreasing as a function of $\rho_Z(h)$. The link's strict monotonicity is known from [23] when G is non-decreasing and differentiable, which does not hold in our case. (Non-strict) monotonicity for arbitrary non-decreasing G is also argued in [7]. Our argument extends strict monotonicity to our setting and identifies an explicit form for the link function's derivative.

Proposition 2.1. *Let $L(\cdot)$ be the link function in (13). Then, for $u \in (-1, 1)$,*

$$L'(u) = \frac{1}{2\pi\gamma_X(0)\sqrt{1-u^2}} \sum_{n_0=0}^{\infty} \sum_{n_1=0}^{\infty} e^{-\frac{1}{2(1-u^2)}(\Phi^{-1}(C_{n_0})^2 + \Phi^{-1}(C_{n_1})^2 - 2u\Phi^{-1}(C_{n_0})\Phi^{-1}(C_{n_1}))}. \quad (30)$$

In particular, $L(u)$ is monotone increasing for $u \in (-1, 1)$.

This result is proven in Appendix A.

Remark 2.7. The antiderivative

$$\int \frac{\exp\left[-\frac{a^2+b^2-2uab}{2(1-u^2)}\right]}{\sqrt{1-u^2}} du$$

does not seem to have a closed form expression for general $a, b \in \mathbb{R}$. (If it did, then one could integrate (30) explicitly and get a closed form expression for $L(u)$.) But a number of numerical ways to evaluate the above integral over a finite interval have been studied; see, for example, [22], Section 2.

2.5 Particle filtering and the HMM connection

This subsection studies the implications of the latent structure of our model, especially as it relates to HMMs and importance sampling approaches. This will be used in constructing particle filtering (PF) approximations of various quantities and in goodness-of-fit

assessments. The first suggested PF approximation of the likelihood below is essentially the popular Geweke-Hajivassiliou-Keane (GHK) sampler for the truncated multivariate normal distribution, and is discussed further in Remark 2.9 below. In general, we closely adhere to the terminology and approaches in the HMM literature.

Our main HMM reference is [16]. As in that monograph, the observations commence at time zero. Let $\hat{Z}_{t+1} = \phi_{t0}Z_t + \dots + \phi_{tt}Z_0$ be the best one-step-ahead linear prediction of Z_{t+1} from Z_0, \dots, Z_t . The weights ϕ_{ts} , $s \in \{0, \dots, t\}$, can be computed recursively in t from the ACVF of $\{Z_t\}$ via the classical Durbin-Levinson (DL) or Innovations algorithm, for example. As a convention, take $\hat{Z}_0 = 0$. Let $r_t^2 = \mathbb{E}[(Z_t - \hat{Z}_t)^2]$ be the corresponding unconditional mean-squared prediction error.

The following problems take center stage:

Filtering : the distribution of \hat{Z}_{t+1} conditional on $X_0 = x_0, \dots, X_t = x_t$,

Prediction : the distribution of X_{t+1} conditional on $X_0 = x_0, \dots, X_t = x_t$,

as well as numerically computing $\mathbb{E}_{\mathcal{H}_t}[V(\hat{Z}_{t+1})]$ and $\mathbb{E}_{\mathcal{H}_t}[V(X_{t+1})]$ for a given function V . Here, $\mathbb{E}_{\mathcal{H}_t}$ indicates an expectation conditioned on the history $\mathcal{H}_t = \{X_0 = x_0, \dots, X_t = x_t\}$. These quantities are needed to evaluate model likelihoods in Section 3.3 and for model diagnostics in Section 3.4.

Our first task is to derive expressions for the above distributions. We use the notation

$$A_k = \{z : \Phi^{-1}(C_{k-1}) \leq z < \Phi^{-1}(C_k)\}, \quad (31)$$

its role stemming from

$$k = G(z) \Leftrightarrow z \in A_k \quad (32)$$

(see (19)). The following result is proven in Appendix A.

Lemma 2.2. *With the above notation and a general function V ,*

$$\mathbb{E}_{\mathcal{H}_t}[V(\hat{Z}_{t+1})] = \frac{\int_{\{z_s \in A_{x_s}, s=0, \dots, t\}} V(\hat{z}_{t+1}) e^{-\frac{1}{2} \sum_{s=0}^t (z_s - \hat{z}_s)^2 / r_s^2} dz_0 \dots dz_t}{\int_{\{z_s \in A_{x_s}, s=0, \dots, t\}} e^{-\frac{1}{2} \sum_{s=0}^t (z_s - \hat{z}_s)^2 / r_s^2} dz_0 \dots dz_t} \quad (33)$$

and

$$\mathbb{E}_{\mathcal{H}_t}[V(X_{t+1})] = \frac{\int_{\mathbb{R}} \int_{\{z_s \in A_{x_s}, s=0, \dots, t\}} V(G(z_{t+1})) e^{-\frac{1}{2} \sum_{s=0}^{t+1} (z_s - \hat{z}_s)^2 / r_s^2} dz_0 \dots dz_{t+1}}{\int_{\mathbb{R}} \int_{\{z_s \in A_{x_s}, s=0, \dots, t\}} e^{-\frac{1}{2} \sum_{s=0}^{t+1} (z_s - \hat{z}_s)^2 / r_s^2} dz_0 \dots dz_{t+1}}. \quad (34)$$

Also,

$$\mathbb{E}_{\mathcal{H}_t}[V(X_{t+1})] = \mathbb{E}_{\mathcal{H}_t}[D_{V,t+1}(\hat{Z}_{t+1})], \quad (35)$$

where, signifying dependence on both V and $t + 1$ as subscripts,

$$D_{V,t+1}(z) = \int_{\mathbb{R}} V(G(z_{t+1})) \frac{e^{-\frac{(z_{t+1}-z)^2}{2r_{t+1}^2}}}{\sqrt{2\pi r_{t+1}^2}} dz_{t+1}. \quad (36)$$

Our filtering algorithm is next described and its connections to the HMM and importance sampling literatures are clarified in subsequent remarks. An additional remark provides insight for those unfamiliar with the HMM literature. The name of the algorithm stems from the HMM connection described in the remarks. Our first result constructs a fair draw of $\{Z_t\}_{t=0}^T$ given the $\{X_t\}_{t=0}^T$ values.

Sequential Importance Sampling (SIS) particle filtering: For $i \in \{1, \dots, N\}$, where N represents the number of particles, initialize the latent series Z_0^i by

$$Z_0^i \stackrel{\mathcal{D}}{=} \left(\mathcal{N}(0, 1) \mid G(\mathcal{N}(0, 1)) = x_0 \right); \quad (37)$$

that is, generate Z_0^i assuming $X_0 = G(Z_0) = x_0$. In view of (32), this is equivalent to generating

$$Z_0^i \stackrel{\mathcal{D}}{=} \left(\mathcal{N}(0, 1) \mid \Phi^{-1}(C_{x_0-1}) \leq \mathcal{N}(0, 1) < \Phi^{-1}(C_{x_0}) \right). \quad (38)$$

Initialize the weight $w_0^i = 1$ and recursively in $t = 1, \dots, T$, perform the following steps:

- 1: Compute \hat{Z}_t^i with the DL or other algorithm and the previously generated values of Z_0^i, \dots, Z_{t-1}^i .
- 2: Sample an error ϵ_t^i conditionally on $X_t = x_t$ via

$$\epsilon_t^i \stackrel{\mathcal{D}}{=} \left(\mathcal{N}(0, 1) \mid G(\hat{Z}_t^i + r_t \mathcal{N}(0, 1)) = x_t \right), \quad (39)$$

or, by (32),

$$\epsilon_t^i \stackrel{\mathcal{D}}{=} \left(\mathcal{N}(0, 1) \mid \frac{\Phi^{-1}(C_{x_{t-1}}) - \hat{Z}_t^i}{r_t} \leq \mathcal{N}(0, 1) < \frac{\Phi^{-1}(C_{x_t}) - \hat{Z}_t^i}{r_t} \right), \quad (40)$$

where $C_{-1} = 0$ by convention.

- 3: Update the Z_t^i series via

$$Z_t^i = \hat{Z}_t^i + r_t \epsilon_t^i \quad (41)$$

and the weights with

$$w_t^i = w_{t-1}^i w_t(\hat{Z}_t^i), \quad (42)$$

where

$$\begin{aligned} w_t(z) &= \int_{A_{x_t}} \frac{e^{-\frac{1}{2r_t^2}(z'-z)^2} dz'}{\sqrt{2\pi r_t^2}} \\ &= \Phi\left(\frac{\Phi^{-1}(C_{x_t}) - z}{r_t}\right) - \Phi\left(\frac{\Phi^{-1}(C_{x_{t-1}}) - z}{r_t}\right). \end{aligned} \quad (43)$$

Then the following approximation can be used:

$$\mathbb{E}_{\mathcal{H}_t}[V(\hat{Z}_{t+1})] \approx \sum_{i=1}^N \frac{w_t^i}{\Omega_{N,t}} V(\hat{Z}_{t+1}^i) = \frac{\frac{1}{N} \sum_{i=1}^N w_t^i V(\hat{Z}_{t+1}^i)}{\frac{1}{N} \sum_{i=1}^N w_t^i} =: \hat{\mathbb{E}}_{\mathcal{H}_t}[V(\hat{Z}_{t+1})], \quad (44)$$

where $\Omega_{N,t} = \sum_{i=1}^N w_t^i$. This approximation is based on the law of large numbers and the IID particles: the limit of the right-hand side of (44) is indeed $\mathbb{E}_{\mathcal{H}_t}[V(\hat{Z}_{t+1})]$. Justification is given in Appendix A.

Proposition 2.2. *In the above notation,*

$$\mathbb{E}_{\mathcal{H}_t}[w_t^i V(\hat{Z}_{t+1}^i)] = \mathbb{E}_{\mathcal{H}_t} \left[V(\hat{Z}_{t+1}^i) \right] \frac{\int_{\{z_s \in A_{x_s}, s=0, \dots, t\}} \frac{e^{-\frac{1}{2} \sum_{s=0}^t (z_s - \hat{z}_s)^2 / r_s^2}}{(2\pi)^{(t+1)/2} r_0 \dots r_t} dz_0 \dots dz_t}{\int_{z_0 \in A_{x_0}} \frac{e^{-z_0^2 / 2}}{(2\pi)^{1/2} r_0} dz_0}. \quad (45)$$

Remark 2.8. The basic idea behind the SIS algorithm is as follows. For $i = 1, \dots, N$, the constructed path $\{Z_t^i\}_{t=0}^T$, is one of the N independent “particles” used to estimate the quantities in (44). For each i , the particle $\{Z_t^i\}_{t=0}^T$ has two keys properties. First, by (41) and (39), it obeys the restriction $G(Z_t^i) = x_t$. Second, it is generated in a way to match the temporal structure of the latent series $\{Z_t\}$ conditional on \mathcal{H}_t , which is ensured through (41). Indeed, note that for an unrestricted $\mathcal{N}(0, 1)$, ϵ_t^i in (41) is the standard way to generate a Gaussian value with the required variance. These two properties show that $\{Z_t^i\}_{t=0}^T$ can be thought as a realization of the latent Gaussian stationary series that produces the observations $X_t = x_t$. While perhaps surprising, unweighted averaging does not lead to an unbiased expected one-step-ahead prediction of the latent Gaussian series given the observations — the weights w_t^i are necessary as shown in the proof of Proposition 2.2. Finally, note where the model parameters enter the SIS algorithm. The marginal distribution parameters $\boldsymbol{\theta}$ enter through the form of C_x in (38), (40), and (43). The temporal dependence parameters $\boldsymbol{\eta}$ enter through the coefficients in the calculation of \hat{Z}_t^i in Step 1 of the algorithm, and through r_t , which arises throughout the algorithm.

Remark 2.9. By (45) and Remark A.1,

$$\mathbb{P}(X_0 = x_0) \mathbb{E}_{\mathcal{H}_T}[w_T^i] = \int_{\{A_{x_s}, s=0, \dots, T\}} \frac{e^{-\frac{1}{2} \sum_{s=0}^T (z_s - \hat{z}_s)^2 / r_s^2}}{(2\pi)^{(t+1)/2} r_0 \dots r_t} dz_0 \dots dz_T \quad (46)$$

$$= \mathbb{P}(X_0 = x_0, \dots, X_T = x_T). \quad (47)$$

The left-hand side of this relation will be used to approximate the model likelihood when using the SIS algorithm. Note further from (42)–(43) that

$$\begin{aligned} w_T^i &= w_1(\hat{Z}_1^i) \cdot \dots \cdot w_T(\hat{Z}_T^i) = \prod_{t=1}^T w_t(\hat{Z}_t^i) \\ &= \prod_{t=1}^T \left[\Phi \left(\frac{\Phi^{-1}(C_{x_t}) - \hat{Z}_t^i}{r_t} \right) - \Phi \left(\frac{\Phi^{-1}(C_{x_{t-1}}) - \hat{Z}_t^i}{r_t} \right) \right]. \end{aligned}$$

Using the sample averages of w_T^i to approximate the truncated multivariate integral on the right-hand side of (46), the procedure can be viewed as the popular GHK sampler ([24], p. 2405). Our contribution is to note that the likelihood can be expressed through the normal integral as in (46)–(47), involving one-step-ahead predictions and their errors, that can be efficiently computed through standard techniques from the time series literature. The GHK sampler is also used in [39], p. 1528, and [26, 27].

The next two remarks and a subsequent discussion further connect our model and algorithm to HMMs and particle filtering.

Remark 2.10. When $\{Z_t\}$ is an AR(p), $(Z_t, \dots, Z_{t-p+1})'$ is a Markov chain on \mathbb{R}^p and our model $X_t = G(Z_t)$ is an HMM (the same conclusion applies to ARMA(p, q) models with an appropriate state space enlargement). Indeed, when $p = 1$, the AR(1) model with a unit variance can be written as $Z_t = \phi Z_{t-1} + (1 - \phi)^{1/2} \epsilon_t$, where $|\phi| < 1$ and $\{\epsilon_t\}$ consists of IID $\mathcal{N}(0, 1)$ random variables. The resulting series $X_t = G(Z_t)$ is then an HMM in the sense of Definition 9.3 in [16] with a Markov kernel on \mathbb{R} given by

$$M(z, dz') = \frac{e^{-\frac{(z' - \phi z)^2}{2(1 - \phi^2)}} dz}{\sqrt{2\pi(1 - \phi^2)}} \quad (48)$$

governing transitions of $\{Z_t\}$, and a Markov kernel from \mathbb{R} to \mathbb{N}_0 ,

$$G(z, dx) = \delta_{G(z)}(dx) = \text{point mass at } G(z) \quad (49)$$

governing the transition from Z_t to X_t . Thus, many of the developments for HMMs (see e.g. Chapters 9–13 in [16]) apply to our model for Gaussian AR(p) $\{Z_t\}$. One important feature of our model when viewed as an HMM is that it is *not* partially dominated (in the sense described following Definition 9.3 in [16]). Though a number of developments described in [16] apply or extend easily to partially non-dominated models (as in the next remark), additional issues need to be addressed for these models.

Remark 2.11. When our model is an HMM with, for example, the underlying Gaussian AR(1) series as in the preceding remark, the algorithm described in (37)–(44) is the Sequential Importance Sampling (SIS) algorithm for particle filtering discussed in Section 10.2 of [16] with the choice of the optimal kernel and the associated weight function in Eqs. (10.30) and (10.31) of [16]. This can be seen from the following observations. For an AR(1) series, the one-step-ahead prediction is $\hat{Z}_{t+1} = \phi Z_t$ (and $\hat{z}_{t+1} = \phi z_t$). Though as noted in the preceding remark, our HMM model is not partially dominated and hence a transition density function $g(z, x)$ (defined following Definition 9.3 of [16]) is not available, a number of formulas for partially dominated HMMs given in [16] also apply to our model by taking

$$g(z, k) = 1_{A_k}(z). \quad (50)$$

This is the case, in particular, for the developments in Section 10.2 on SIS in [16]. For example, one could check with (50) that the filtering distribution of ϕ_t in Eq. (10.23) of [16] is exactly that in (33). The kernel $Q_t(z, A)$ appearing in Section 10.2 of [16] is then

$$Q_t(z, A) = \int_A M(z, dz') g(z', x_t) = \int_{A \cap A_{x_t}} \frac{e^{-\frac{(z' - \phi z)^2}{2(1 - \phi^2)}} dz'}{\sqrt{2\pi(1 - \phi^2)}}, \quad (51)$$

where (48) and (50) were used. Sampling Z_t^i from the optimal kernel $Q_t(Z_{t-1}^i, \cdot) / Q_t(Z_{t-1}^i, \mathbb{R})$ (see p. 330 in [16]) can be shown to be equivalent to defining Z_t^i through Steps 2 and 3 of our particle filtering algorithm above. The optimal weight function $Q_t(z, \mathbb{R})$ can also be checked to be that in (43) above.

Following particle filtering developments in the HMM literature (Sections 10.4.1 and 10.4.2 in [16]), our SIS algorithm could be modified into the following two algorithms. In fact, the SISR algorithm below is used whenever the sample size T is larger; specifically, all Section 4 simulations use this. For larger T , the particles in the SIS algorithm “degenerate” in the following sense. Note from (42) that the weights w_t^i are defined as cumulative products of the multiplicative factors $w_s(\hat{Z}_s^i)$ over $s \leq t-1$. But each $w_s(\cdot)$, being a probability according to (43), is between 0 and 1. With hundreds of such multiplicative factors, their cumulative products defining the weight becomes small numerically.

Sequential Importance Sampling with Resampling (SISR) particle filtering: Proceed as in the SIS algorithm, but modify Step 3 and add a resampling Step 4 as follows:

3: Modify Step 3 of the SIS by setting

$$\tilde{Z}_t^i = \hat{Z}_t^i + r_t \epsilon_t^i, \quad \tilde{w}_t^i = w_{t-1}^i w_t(\hat{Z}_t^i) \quad (52)$$

and also $\tilde{\Omega}_{N,t} = \sum_{i=1}^N \tilde{w}_t^i$.

4: Draw, conditionally and independently given $\{(Z_s^i, w_s^i), s \leq t-1, i = 1, \dots, N\}$ and $\{\tilde{Z}_t^i, i = 1, \dots, N\}$, a multinomial trial $\{I_t^i, i = 1, \dots, N\}$ with probabilities of success $\{\tilde{w}_t^i / \tilde{\Omega}_{N,t}\}$ and set $Z_t^i = \tilde{Z}_t^{I_t^i}$ and $w_t^i = 1, i \in \{1, \dots, N\}$.

The resampling step removes particles with low weights, mitigating degeneracy issues, but may increase estimator variance. For this reason, we follow standard practice and resample only when the variance of the weights exceeds a certain threshold. The variability of the weights is quantified by the so-called *effective sample size* defined as

$$\text{ESS}(w_t^i) = \left(\sum_{i=1}^N \left(\frac{w_t^i}{\Omega_{N,t}} \right)^2 \right)^{-1}.$$

For our simulations and data applications, standard practice is followed in that resampling is triggered when $\text{ESS} < \epsilon N$, where $\epsilon = 0.5$.

Auxiliary particle filtering (APF): Proceed as in the SIS algorithm, but modify Step 3 as follows:

3: Denote the distribution of Z_t^i in (41) as $R_t(\hat{Z}_t^i, \cdot)$. Then, draw conditionally independently pairs $\{(I_t^i, Z_t^i), i = 1, \dots, N\}$ of indices and particles from the distribution

$$\mu(\{i\} \times A) = \frac{w_t(\hat{Z}_t^i)}{\sum_{i=1}^N w_t(\hat{Z}_t^i)} R_t(\hat{Z}_t^i, A), \quad (53)$$

where $w_t(z)$ is defined in (43). Discard the indices to take $\{Z_t^i, i = 1, \dots, N\}$ for the particles at time t . Also, set $w_t^i = 1$ for all $i \in \{1, \dots, N\}$.

Finally, we turn to prediction, namely, evaluating $\mathbb{E}_{\mathcal{H}_t}[V(X_{t+1})]$. This can be addressed by relating prediction to the filtering problem as in (35). For example, when using SIS particle filtering, approximate $\mathbb{E}_{\mathcal{H}_t}[V(X_{t+1})]$ via

$$\mathbb{E}_{\mathcal{H}_t}[V(X_{t+1})] \approx \sum_{i=1}^N \frac{w_t^i}{\Omega_{N,t}} D_{V,t+1}(\hat{Z}_{t+1}^i) \quad (54)$$

(see (44) and (35)–(36)). The SISR and APF algorithms could also be used.

3 Inference

The model in (1) contains the parameters $\boldsymbol{\theta}$ in the marginal count distribution F_X and the parameters $\boldsymbol{\eta}$ governing the dependence structure in $\{Z_t\}$. This section addresses inference questions, including parameter estimation and goodness-of-fit assessment. Three methods are presented for parameter estimation: Gaussian pseudo-likelihood, implied Yule-Walker moment methods, and full likelihood. Gaussian pseudo-likelihood estimators, a time series staple, are obtained by pretending the series is Gaussian and maximizing its Gaussian likelihood. These estimators only involve the mean and covariance structure of the series, are easy to compute, and will provide a comparative basis for likelihood estimators. Implied Yule-Walker techniques are moment based estimators for the commonly encountered case where $\{Z_t\}$ is a causal autoregression. Likelihood estimators, the statistical gold standard and the generally preferred estimation technique, are based on the particle filtering methods of the last section.

3.1 Gaussian pseudo-likelihood estimation

As in Section 2.5, we assume observations x_t for times $t \in \{0, \dots, T\}$ and set $\mathbf{X} = (x_0, \dots, x_T)'$. Denote the likelihood of the model in (1) by

$$\mathcal{L}_T(\boldsymbol{\theta}, \boldsymbol{\eta}) = \mathbb{P}(X_0 = x_0, X_1 = x_1, \dots, X_T = x_T). \quad (55)$$

While this likelihood is just a multivariate normal probability, it is difficult to calculate or approximate when T is large. For most count model classes, true likelihood estimation is difficult as joint distributions are generally intractable [14]. While Section 3.3 below devises a particle filtering likelihood approximation [47], for comparative purposes, we first consider a simple Gaussian pseudo-likelihood (GL) approach. In a pseudo GL approach, parameters are estimated via

$$(\hat{\boldsymbol{\theta}}, \hat{\boldsymbol{\eta}}) = \underset{\boldsymbol{\theta}, \boldsymbol{\eta}}{\operatorname{argmax}} \frac{e^{-\frac{1}{2}(\mathbf{X} - \boldsymbol{\mu}_{\boldsymbol{\theta}})' \Gamma_T(\boldsymbol{\theta}, \boldsymbol{\eta})^{-1} (\mathbf{X} - \boldsymbol{\mu}_{\boldsymbol{\theta}})}}{(2\pi)^{(T+1)/2} |\Gamma_T(\boldsymbol{\theta}, \boldsymbol{\eta})|^{1/2}}, \quad (56)$$

where $\boldsymbol{\mu}_{\boldsymbol{\theta}} = (\mu_{\boldsymbol{\theta}}, \dots, \mu_{\boldsymbol{\theta}})'$ is a $(T + 1)$ -dimensional constant mean vector. These estimators maximize the series' likelihood assuming the data are Gaussian, each component having mean $\mu_{\boldsymbol{\theta}}$, and all components having covariance matrix $\Gamma_T(\boldsymbol{\theta}, \boldsymbol{\eta}) = (\gamma_X(i - j))_{i,j=0}^T$. Time series analysts have been maximizing Gaussian pseudo likelihoods for decades, regardless of the series' marginal distribution, with often satisfactory performance. In the next section, simulations provide a case where this approach works reasonably well, and one where it does not. For large T , the pseudo GL approach is equivalent to least squares, where the sum of squares

$$\sum_{t=0}^T (X_t - \mathbb{E}[X_t | X_0, \dots, X_{t-1}])^2$$

is minimized (see Chapter 8 in [6]). The covariance structure of $\{X_t\}$ was efficiently computed in Section 2; the mean $\mu_{\boldsymbol{\theta}}$ is usually explicitly obtained from the marginal distribution

posed. Numerical optimization of (56) yields a Hessian matrix that can be inverted to obtain standard errors for the model parameters. These standard errors can be asymptotically corrected for distributional misspecification via the sandwich methods of [21].

3.2 Implied Yule-Walker estimation for latent AR models

Suppose that $\{Z_t\}$ follows the causal AR(p) model

$$Z_t = \phi_1 Z_{t-1} + \dots + \phi_p Z_{t-p} + \varepsilon_t, \quad (57)$$

where $\{\varepsilon_t\}$ consists of IID $\mathcal{N}(0, \sigma_\varepsilon^2)$ variables. Here, σ_ε^2 depends on ϕ_1, \dots, ϕ_p in a way that induces $\mathbb{E}[Z_t^2] = 1$. The Yule-Walker equations are

$$\boldsymbol{\phi} = \boldsymbol{\Gamma}_p^{-1} \boldsymbol{\gamma}_p, \quad (58)$$

where $\boldsymbol{\Gamma}_p = (\gamma_Z(i-j))_{i,j=1}^p$, $\boldsymbol{\gamma}_p = (\gamma_Z(1), \dots, \gamma_Z(p))'$ and $\boldsymbol{\phi} = (\phi_1, \dots, \phi_p)'$. From (12), note that

$$\gamma_Z(h) = L^{-1}(\rho_X(h)), \quad (59)$$

the inverse being justified via the strictly increasing nature of $L(u)$ in u .

Equations (58) and (59) suggest the following estimation procedure. First, estimate the CDF parameter $\boldsymbol{\theta}$ directly from the counts themselves through any standard method. The estimated parameter $\hat{\boldsymbol{\theta}}$ defines the estimated link $\hat{L}(u)$ through its estimated power series coefficients. From a numerical power series reversion procedure (e.g. [28]), one can now efficiently construct the inverse estimator $\hat{L}^{-1}(\rho)$.

Next, in view of (59), set

$$\hat{\gamma}_Z(h) = \hat{L}^{-1}(\hat{\rho}_X(h)), \quad (60)$$

where $\hat{\rho}_X(h)$ refers to the lag- h sample ACF of $\{X_t\}$. From (58), we estimate the unknown AR coefficients via

$$\hat{\boldsymbol{\phi}} = \hat{\boldsymbol{\Gamma}}_p^{-1} \hat{\boldsymbol{\gamma}}_p, \quad (61)$$

where $\hat{\boldsymbol{\Gamma}}_p$ and $\hat{\boldsymbol{\gamma}}_p$ are defined analogously using (60).

3.3 Particle filtering likelihood approximations

Using the notation and results leading to (35) in Lemma 2.2, the true likelihood in (55) is

$$\begin{aligned} \mathcal{L}_T(\boldsymbol{\theta}, \boldsymbol{\eta}) &= \mathbb{P}(X_0 = x_0) \prod_{s=1}^T \mathbb{P}(X_s = x_s | X_0 = x_0, \dots, X_{s-1} = x_{s-1}) \\ &= \mathbb{P}(X_0 = x_0) \prod_{s=1}^T \mathbb{E}_{\mathcal{H}_{s-1}}[1_{\{x_s\}}(X_s)] \\ &= \mathbb{P}(X_0 = x_0) \prod_{s=1}^T \mathbb{E}_{\mathcal{H}_{s-1}}[w_s(\hat{Z}_s)], \end{aligned} \quad (62)$$

where (36) was used with $D_{1_{\{x_s\}},s}(z) = w_s(z)$ and $w_s(z)$ is defined and numerically computed akin to (43). The particle approximation of the likelihood is then

$$\hat{\mathcal{L}}_T(\boldsymbol{\theta}, \boldsymbol{\eta}) = \mathbb{P}(X_0 = x_0) \prod_{s=1}^T \hat{\mathbb{E}}_{\mathcal{H}_{s-1}}[w_s(\hat{Z}_s)]; \quad (63)$$

this uses the notation in (44) and supposes that the particles are generated by one of the methods in Section 2.5. The particle approximation MLEs satisfy

$$(\hat{\boldsymbol{\theta}}, \hat{\boldsymbol{\eta}}) = \underset{\boldsymbol{\theta}, \boldsymbol{\eta}}{\operatorname{argmax}} \hat{\mathcal{L}}_T(\boldsymbol{\theta}, \boldsymbol{\eta}). \quad (64)$$

Remark 3.1. With the SIS algorithm, (63) reduces to

$$\hat{\mathcal{L}}_T(\boldsymbol{\theta}, \boldsymbol{\eta}) = \mathbb{P}(X_0 = x_0) \frac{1}{N} \sum_{i=1}^N w_T^i, \quad (65)$$

which is consistent with Remark 2.9. As stated in that remark, [39, 40, 26] also essentially implement (65). In fact, our model can also be fitted for a number of marginal distributions and correlation structures with the *R* package *gcmr* of [40]. The current implementation of *gcmr*, however, only allows for marginal distributions within the generalized linear model (GLM, for short) framework (and the *glm* function in *R*), and thus must come from the exponential family; see, in particular, Appendix A.1 in [40]. In our implementation, any parametric marginal distribution can be accommodated, including those not from the exponential family; for example, a mixture Poisson distribution is considered in Section 4 below. Furthermore, unlike the *gcmr* package, pseudo GL and implied Yule-Walker estimation are also considered. We also provide model diagnostics tools more specific to count series, such as PIT histograms in Section 3.4 below.

In optimizing $\hat{\mathcal{L}}_T(\boldsymbol{\theta}, \boldsymbol{\eta})$, a common practice, as used in the *gcmr* package of [40] and *gcKrig* of [26] and known as Common Random Numbers (CRNs), expresses the random quantities in particle filtering methods through transformations (depending on model parameters) of uniform random variables and then keep the latter constant across likelihood approximations for different parameter values. This CRN procedure ensures that the likelihood $\hat{\mathcal{L}}_T(\boldsymbol{\theta}, \boldsymbol{\eta})$ is smooth over its parameters. Alternatively, the “noisy” likelihood $\hat{\mathcal{L}}_T(\boldsymbol{\theta}, \boldsymbol{\eta})$ without CRNs can be optimized by global optimization methods (e.g., as in *R* package *DEoptim* [1, 44] implementing the method in [49] akin to particle optimization), but this is often considerably slower.

3.4 Model diagnostics

The goodness-of-fit of count models is commonly assessed through probability integral transform (PIT) histograms and related tools [11, 35]. These are based on the predictive distributions of $\{X_t\}$, defined at time t by

$$P_t(y) = \mathbb{P}_{\mathcal{H}_{t-1}}(X_t \leq y) = \mathbb{P}(X_t \leq y | X_0 = x_0, \dots, X_{t-1} = x_{t-1}), \quad y \in \{0, 1, \dots\}. \quad (66)$$

This quantity can be estimated through the particle filtering methods in Section 2.5:

$$\hat{P}_t(y) = \sum_{x=0}^y \hat{\mathbb{E}}_{\mathcal{H}_{t-1}}[1_{\{x\}}(X_t)] = \sum_{x=0}^y \hat{\mathbb{E}}_{\mathcal{H}_{t-1}}[D_{1_{\{x\}},t}(\hat{Z}_t)], \quad (67)$$

which uses (36) and (44) and supposes that the particles are generated by the SIS, SISR, or APF algorithms. Similar to $D_{1_{\{x_s\}},s}(z) = w_s(z)$, note that $D_{1_{\{x\}},t}(z) = \tilde{w}_{x,t}(z)$, where

$$\tilde{w}_{x,t}(z) = \Phi\left(\frac{\Phi^{-1}(C_x) - z}{r_t}\right) - \Phi\left(\frac{\Phi^{-1}(C_{x-1}) - z}{r_t}\right) \quad (68)$$

(and $\tilde{w}_{x,t}(z) = w_t(z)$).

The (non-randomized) mean PIT is defined as

$$\bar{F}(u) = \frac{1}{T+1} \sum_{t=0}^T F_t(u|x_t), \quad u \in [0, 1], \quad (69)$$

where

$$F_t(u|y) = \begin{cases} 0, & \text{if } u \leq P_t(y-1), \\ \frac{u-P_t(y-1)}{P_t(y)-P_t(y-1)}, & \text{if } P_t(y-1) < u < P_t(y), \\ 1, & \text{if } u \geq P_t(y), \end{cases} \quad (70)$$

which is estimated by replacing P_t by \hat{P}_t in practice. The PIT histogram with H bins is defined as a histogram with the height $\bar{F}(h/H) - \bar{F}((h-1)/H)$ for bin $h \in \{1, \dots, H\}$.

As a more elementary diagnostic tool, another possibility considers model residuals defined as

$$\hat{Z}_t = \mathbb{E}(Z_t|X_t = x_t) = \frac{\exp(-\Phi^{-1}(C_{x_{t-1}})^2/2) - \exp(-\Phi^{-1}(C_{x_t})^2/2)}{\sqrt{2\pi}(C_{x_t} - C_{x_{t-1}})}, \quad (71)$$

which is the estimated mean of the latent Gaussian process at time t given X_t only (not the entire past), where the formula (71) follows by direct calculations for the model (1) (assuming the estimated parameter values $\boldsymbol{\theta}$ of the marginal distribution entering C_{kS}). For a fitted underlying time series model with parameter $\boldsymbol{\eta}$, the residuals are then defined as the residuals $\hat{\epsilon}_t$ of this model fitted to the series \hat{Z}_t , after centering by the sample mean. In more formal terms (omitting the sample mean for simplicity),

$$\hat{\epsilon}_t = \hat{Z}_t - \mathbb{E}_{\boldsymbol{\eta}}(\hat{Z}_t|\hat{Z}_{t-1}, \dots, \hat{Z}_0),$$

where $\mathbb{E}_{\boldsymbol{\eta}}$ denotes a linear prediction under the fitted time series model with parameter $\boldsymbol{\eta}$.

3.5 Nonstationarity and covariates

As discussed in Section 2.2, covariates can be accommodated in the model via a time-varying $\boldsymbol{\theta}$ parameter in the marginal distribution. With covariates, $\boldsymbol{\theta}$ at time t is denoted by $\boldsymbol{\theta}(t)$. The GL and particle inference procedures are modified for $\boldsymbol{\theta}(t)$ as follows.

For the GL procedure, the covariance $\text{Cov}(X_{t_1}, X_{t_2}) = \text{Cov}(G_{\boldsymbol{\theta}(t_1)}(Z_{t_1}), G_{\boldsymbol{\theta}(t_2)}(Z_{t_2}))$ is needed, where $\boldsymbol{\theta}(t)$ is subscripted on G to signify dependence on t . But as in (9),

$$\text{Cov}(X_{t_1}, X_{t_2}) = \text{Cov}(G_{\boldsymbol{\theta}(t_1)}(Z_{t_1}), G_{\boldsymbol{\theta}(t_2)}(Z_{t_2})) = \sum_{k=1}^{\infty} k! g_{\boldsymbol{\theta}(t_1),k} g_{\boldsymbol{\theta}(t_2),k} \gamma_Z(t_1 - t_2)^k, \quad (72)$$

where again, the subscript $\boldsymbol{\theta}(t)$ is added to g_k to indicate dependence on t . Numerically, evaluating (72) is akin to that in (9); in particular, both calculations are based on the Hermite coefficients $\{g_k\}$.

For the particle filtering approach, the modification is somewhat simpler: one just needs to replace $\boldsymbol{\theta}$ by $\boldsymbol{\theta}(t)$ at time t when generating the underlying particles. For example, for the SIS algorithm, $\boldsymbol{\theta}(t)$ would enter through C_x in (38), (40), and (43). This modification is justified from the structure of the model, where the covariates enter only through the parameter $\boldsymbol{\theta}$ controlling the marginal distribution.

4 A simulation study

To assess the performance of our estimation methods, a simulation study considering several marginal distributions and dependence structures was conducted. Here, Poisson, mixed Poisson, and negative binomial count distributions are examined, with underlying ARMA(p, q) $\{Z_t\}$ processes. All simulation cases are replicated 200 times for three distinct series lengths: $T = 100, 200$, and 400 . For notation, estimates of a parameter ζ from Gaussian pseudolikelihood (GL), implied Yule-Walker (IYW), and particle filtering (PF) methods are denoted by $\hat{\zeta}_{GL}$, $\hat{\zeta}_{IYW}$, and $\hat{\zeta}_{PF}$, respectively. The CDFs of the three distributions are denoted by \mathcal{P} , \mathcal{MP} , and \mathcal{NB} .

4.1 Poisson AR(1)

We begin with the simple case where X_t has a Poisson marginal distribution for each t with mean $\lambda > 0$. To obtain X_t , the AR(1) process

$$Z_t = \phi Z_{t-1} + (1 - \phi^2)^{1/2} \epsilon_t, \quad (73)$$

was simulated and transformed via (1)–(2) with $F = \mathcal{P}$; $\mathbb{E}[Z_t^2] \equiv 1$ was induced by taking $\sigma_\epsilon^2 = (1 - \phi^2)^{-1}$. Twelve parameter schemes resulting from all combinations of $\lambda \in \{2, 5, 10\}$ and $\phi \in \{\pm 0.25, \pm 0.75\}$ were considered.

Figure 3 displays box plots of the parameter estimates when $\lambda = 2$. In estimating λ , all methods perform reasonably well. When the lag-one correlation in $\{Z_t\}$ (and hence also that in $\{X_t\}$) is negative (right panel), $\hat{\lambda}_{GL}$, $\hat{\lambda}_{IYW}$, and $\hat{\lambda}_{PF}$ have smaller variability than the positively correlated case (left panel — note the different y-axis scales on the panels). This is expected: the mean of $\{X_t\}$ is λ , and the variability of the sample mean, one good estimator of the mean for a stationary series, is smaller for negatively correlated series than for positively correlated ones. Moreover, the estimates $\hat{\lambda}_{GL}$ from negatively correlated series have smaller biases than their positively correlated counterparts. Note that $\hat{\phi}_{GL}$ and $\hat{\phi}_{IYW}$ are biased toward zero for both negatively and positively correlated series, while the PF estimates

generally show less bias. All estimates of ϕ have roughly similar variances. Simulations with $\lambda = 5$ and $\lambda = 10$ produced analogous results with smaller values of λ yielding less variable estimates. This is again expected as the variance of the Poisson distribution is also λ . These box plots are omitted for brevity's sake.

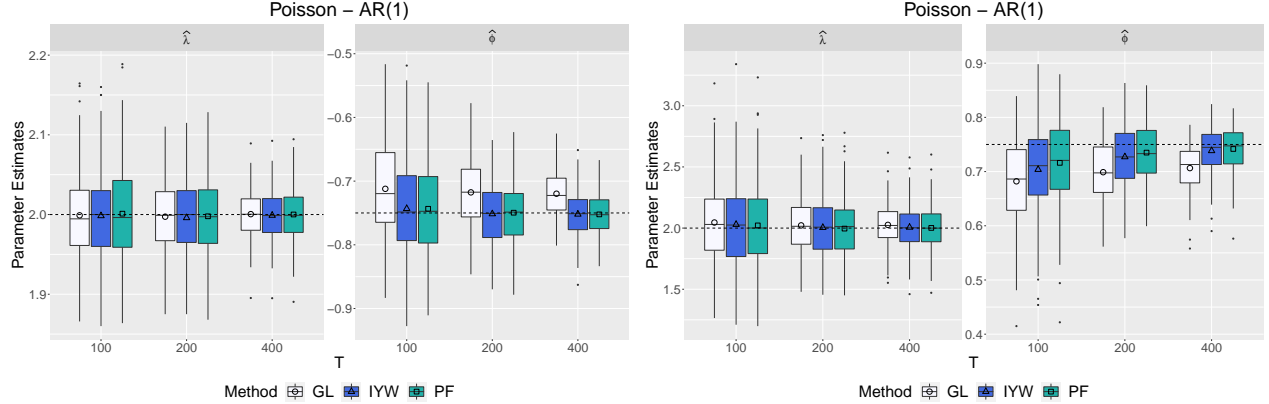


Figure 3: Gaussian likelihood, implied Yule-Walker, and particle filtering parameter estimates for 200 synthetic Poisson-AR(1) series with lengths $T = 100, 200$, and 400 . The true parameter values (indicated by the black horizontal dashed lines) are $\lambda = 2$, $\phi = 0.75$ (left panel), and $\lambda = 2$ and $\phi = -0.75$ (right panel).

4.2 Mixed Poisson AR(1)

We next consider the three-parameter mixture Poisson marginal distribution with parameters $\lambda_1 > 0$, $\lambda_2 > 0$, and $p \in [0, 1]$, and probability mass function as defined in Section 2. As in Section 4.1, the count series was obtained by transforming (73) via (1)–(2) with $F = \mathcal{MP}$. Eight parameter schemes that consider all combinations of $\lambda_1 = 2$, $\lambda_2 \in \{5, 10\}$, $p = 0.25$, and $\phi = \{\pm 0.25, \pm 0.75\}$ are studied.

Figure 4 shows box plots of the parameter estimates for $\phi = 0.75$ and $\lambda_2 = 5$ or 10 (left or right panels, respectively). To ensure parameter identifiability, p was constrained to lie in $(0, 1/2)$. In the $\lambda_2 = 5$ case (left panel), PF methods outperform GL and IYW approaches, yielding smaller biases and variances for most parameter choices and all sample sizes. The only exception occurs with λ_2 , where $\hat{\lambda}_{2,GL}$ were moderately superior to $\hat{\lambda}_{2,PF}$ and $\hat{\lambda}_{2,IYW}$ for $T = 100$ and $T = 200$; however for $T = 400$, PF performs well, having little bias and the smallest variance of the three methods. IYW produced significantly smaller biases than GL in estimating λ_1 and p , but both methods estimate ϕ somewhat biasedly. IYW also displays larger variances for estimates of λ_1 , λ_2 , and p when T is smaller.

In the $\lambda_2 = 10$ case (right panel), where bimodality features are more pronounced, the GL method performs (as one might expect) quite poorly. Here, the probability that X_t is close to its mean value of $p\lambda_1 + (1-p)\lambda_2$ is actually quite small, but GL overestimates it as the mode of the corresponding Gaussian distribution with that mean. In contrast, the PF approach feels the entire joint distribution of the process, outperforming the IYW and GL approaches across the board. IYW also does reasonably well in this setting, although not quite as good as PF.

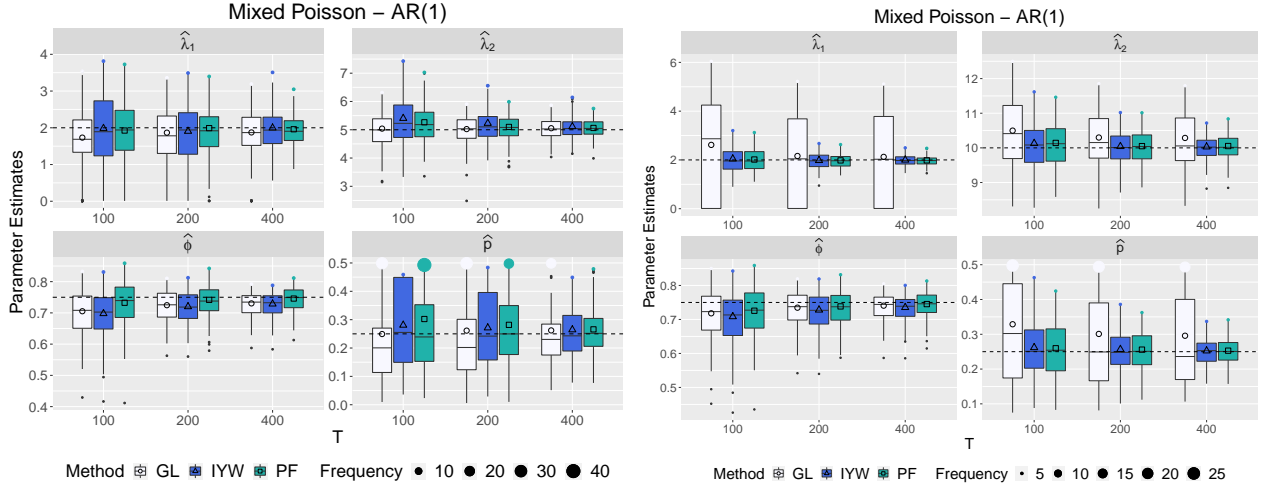


Figure 4: Gaussian likelihood, implied Yule-Walker, and particle filtering parameter estimates for 200 synthetic mixed Poisson AR(1) series of lengths $T = 100, 200$, and 400 . The true parameter values (indicated by the black horizontal dashed lines) are $\lambda_1 = 2$, $\lambda_2 = 5$, $\phi = 0.75$, and $p = 1/4$ (left panel) and $\lambda_1 = 2$, $\lambda_2 = 10$, $\phi = 0.75$, and $p = 1/4$ (right panel).

4.3 Negative binomial MA(1)

Our final case considers the negative binomial distribution with parameters $r > 0$, and $p \in (0, 1)$ and probability mass function as defined in Section 2. To obtain X_t , the MA(1) process

$$Z_t = \epsilon_t + \theta \epsilon_{t-1}, \quad (74)$$

was simulated and transformed via (1)–(2) with $F = \mathcal{NB}$; $\mathbb{E}[Z_t^2] \equiv 1$ was induced by taking $\sigma_\epsilon^2 = (1 + \theta^2)^{-1}$. Eight parameter schemes resulting from all combinations of $p \in \{0.2, 0.5\}$, $r = 3$, and $\theta \in \{\pm 0.25, \pm 0.75\}$ were considered. The negative binomial marginal distribution is overdispersed. Since $\{Z_t\}$ is not an autoregression, IYW estimates are not considered.

Figure 5 displays box plots of parameter estimates from models with $\theta = 0.75$ (left panel) and $\theta = -0.75$ (right panel). The PF approach is clearly the superior method here for all parameters and sample sizes. GL estimates display ‘‘boundary issues’’ for $\hat{\theta}_{GL}$ for small T and negatively correlated series (right panel). Elaborating, we impose $\hat{\theta}$ to lie in $(-1, 1)$ for an invertible moving-average and some GL runs ‘‘press this estimate’’ out to -1 . GL boundary issues (and any biases) dissipate and sampling variability decreases appreciably with the largest series length $T = 400$; this said, PF still performs best.

Overall, PF likelihood methods exhibit the best performance, with the simple moment IYW methods being serviceable in the case where $\{Z_t\}$ is an autoregression. PF techniques were also recommended by [27] (compared to other likelihood approximations) in spatial settings.

We conclude this section with a description of an ANOVA-type experiment that was conducted to numerically quantify the PF approximation error and compare its magnitude against estimation bias. Specifically, our simulation study fitted each realization (from a total of 200) of a Poisson-AR(12) model five times (we do not list the chosen AR coefficients, but results are reasonably robust to their choice). For each fit, the particle numbers $N \in$

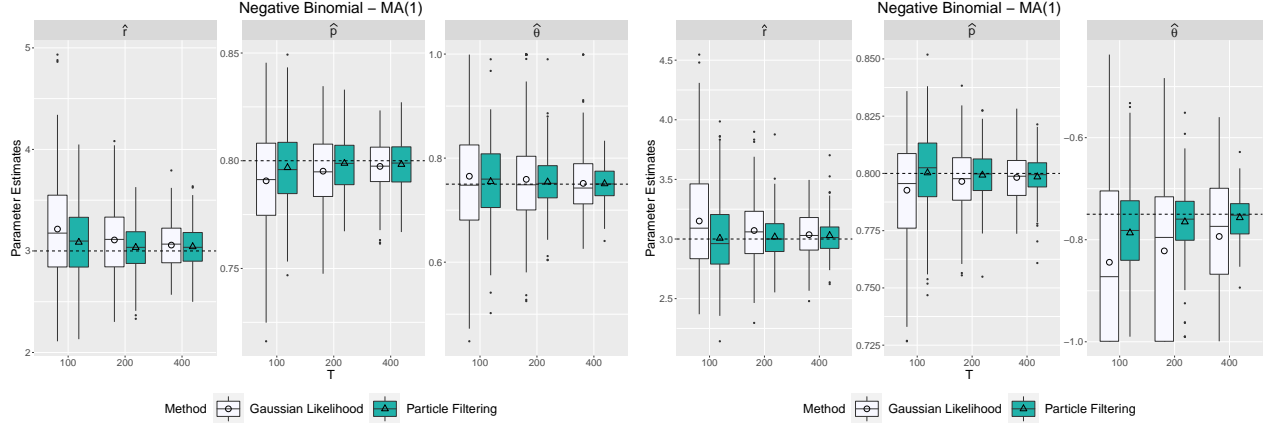


Figure 5: Gaussian likelihood and particle filtering parameter estimates for 200 synthetic negative binomial MA(1) series of lengths $T = 100, 200$ and 400 . The true parameter values (indicated by the black horizontal dashed lines) are $r = 3$, $p = 0.2$ and $\theta = 0.75$ (left panel) and $r = 3$, $p = 0.2$ and $\theta = -0.75$ (right panel).

$\{5, 10, 100, 500\}$ are considered. For each N , the 200 5-tuples of parameter estimates can be viewed as 200 ANOVA treatments, where the between- and within-treatments variations quantify the estimation and approximation error respectively. We found that the estimation error dominated the PF approximation error by several orders of magnitude, even for the smallest number of particles. While detailed results are omitted for brevity's sake, the inference is that the PF likelihood approximation is reasonably accurate.

5 An application

This section applies our methods to a weekly count series of product sales at Dominick's Finer Foods, a now defunct U.S. grocery chain that operated in Chicago, IL and adjacent areas from 1918 - 2013. Soft drink sales of a particular brand from a single store will be analyzed over a two-year span commencing on September 10, 1989. The series is plotted in Figure 6 (top plot) and is part of a large and well-studied retail dataset, publicly available at <https://www.chicagobooth.edu/research/kilts/datasets/dominicks> (Source: The James M. Kilts Center for Marketing, University of Chicago).¹ The goal here is to illustrate our methods with a real world example of an overdispersed time series of small counts that exhibit negative autocorrelation and significant dependence on a covariate.

The covariate here is a binary zero-one “buy one get one free” (BOGO for short) sales promotion event S_t , $S_t = 1$ implying that the BOGO promotion was offered at least one day during week t . The blue dots in the top plot of Figure 6 signify that the week had at least one BOGO day. The bottom left plot of Figure 6 shows the soft drinks sales distribution grouped by S_t , visually suggesting that a BOGO event increases soft drink sales. The bottom middle and right plots of Figure 6 display the sample ACF and PACF of the series and show

¹In the dataset manual, the series in Figure 6 (top plot) is the sales of the product with universal product code (UPC) 4640055081 from store 81.

negative dependence at lag one. The lag one sample autocorrelation of the residuals from the regression of the series on the BOGO covariate is also negative, but comparatively smaller in magnitude.

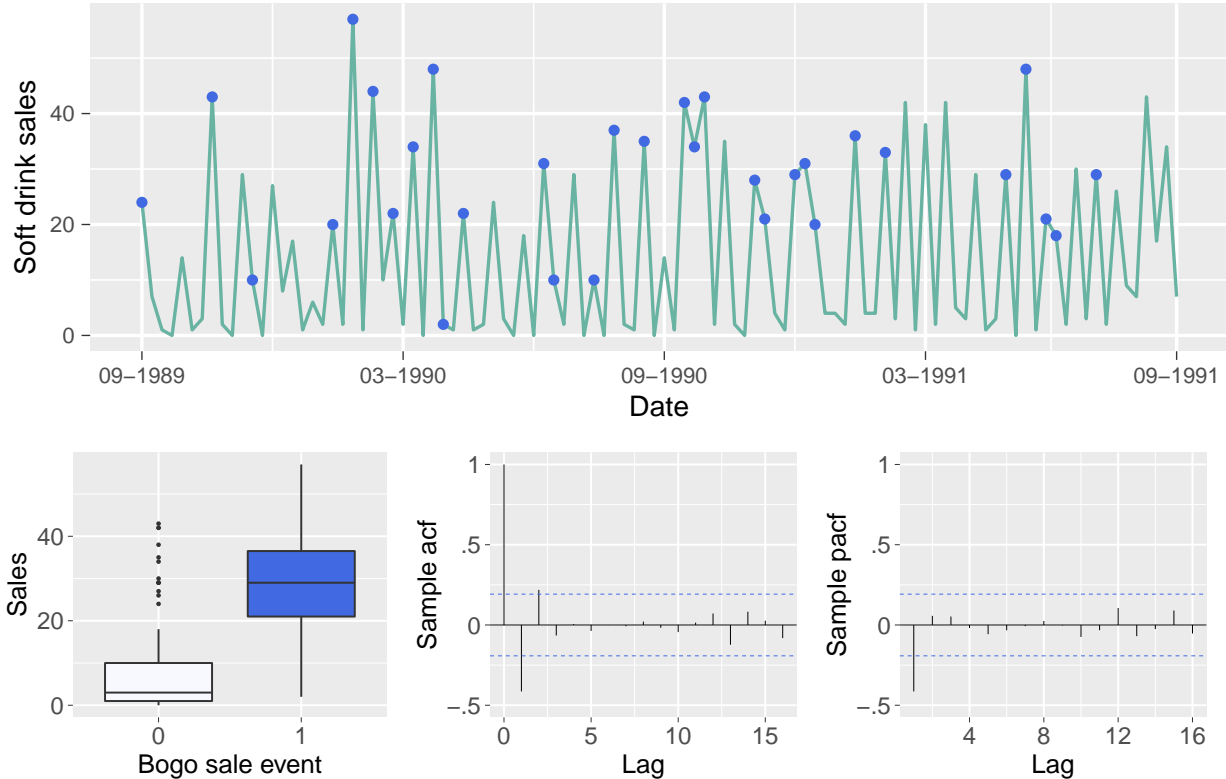


Figure 6: Top: Weekly sales of a soft drink product sold at a single store of the grocery store *Dominick's Finer Foods* from September 10, 1989 to September 3, 1991. The blue dots indicate the weekly sales were at least one “Buy one and get one free” (BOGO) sales promotion event took place. Bottom left: Boxplots of sales grouped by the BOGO covariate (0: weekly sales with no BOGO event, 1: weekly sales with at least one BOGO day during the week). Bottom middle and right: Sample ACF and PACF plots of the series.

To capture the overdispersion of the counts, negative binomial and generalized Poisson marginal distributions will be considered. Although similar, these two distributions can yield different fits (see, for example, [33] and [45]). Following standard GLM practices, both distributions are parametrized via the series’ mean (although our model allows covariates to enter through other parameters as well). More specifically, for the negative binomial marginal, the standard pair (r, p) used in Section 4 is now mapped to the parameter pair (μ, k) , where $\mu = pr/(1 - p)$ is the mean of the process and $k = 1/r$ is the overdispersion parameter. Similarly, the generalized Poisson distribution of Section 2 is parametrized through the pair (μ, α) as in [17], relation (2.4). Here, μ is the mean of the series, whereas the sign of the parameter α controls the type of dispersion, with positive values indicating overdispersion.

To incorporate the BOGO covariate S_t into the model, the mean of the series is allowed

to depend on time t through the typical GLM log-link

$$\mu_t = \exp(\beta_0 + \beta_1 S_t),$$

while the parameters k and α are kept fixed in time t .

Marginal Distribution	Model	WN	AR(1)	AR(2)	AR(3)	MA(1)	MA(2)	MA(3)
negative binomial	AICc_{GL}	844.2	827.5	828.4	829.9	834.2	825.4	825.4
	BIC_{GL}	851.9	837.7	841.0	844.9	844.4	838	840.4
	AICc_{PF}	748.5	736.9	732.0	721.7	741.5	730.3	729.9
	BIC_{PF}	756.2	747.1	744.6	736.7	751.7	742.9	744.9
generalized Poisson	AICc_{GL}	847.5	830.6	831.0	833.3	836.9	828.7	828.6
	BIC_{GL}	855.2	840.8	843.6	848.3	847.0	841.3	843.6
	AICc_{PF}	769.2	754.1	749.8	741.2	758.6	749.8	749.9
	BIC_{PF}	776.9	764.3	762.4	756.2	768.8	762.4	764.9

Table 1: AIC and BIC statistics for generalized Poisson and negative binomial distributions with different latent Gaussian ARMA orders.

An exploratory examination of the sample ACFs and PACFs of the series along with diagnostic plots of residuals obtained by fitting all $\text{ARMA}(p, q)$ models with $p, q \leq 3$ suggest an AR(3) model as a suitable choice. Table 1 shows the AIC and BIC for both marginal distributions obtained via PF and GL methods (we omit the IYW throughout the section for simplicity). The AR(3) model was selected by the AICc and BIC for both PF fits. Interestingly, both the sample ACF and PACF of the series show one large non-zero autocovariance at lag one, but relatively smaller values at other lags (except perhaps the lag two autocorrelation, which barely exceeds the 95% $1.96/\sqrt{T}$ dashed blue confidence threshold for zero correlation).

We also considered a white noise latent series (labeled as “WN” in the first column of Table 1), which reduces our model to a standard GLM. The particle filter WN estimates from both distributions (omitted here for brevity) approximated closely the parameter estimates we obtained from exact GLM fits (using, for example, functions from the R package “MASS”). As expected, the WN model yielded the highest AICc and BIC values amongst all considered dependence structures, thus confirming the need for a model that allows for temporal dependence.

Tables 2 and 3 show parameter estimates and standard errors from fitting a negative binomial-AR(3) and a generalized Poisson-AR(3) model. All marginal distributions and estimation methods yielded $\hat{\phi}_1 < 0$. Although a formal asymptotic theory is beyond the scope of our presentation here, asymptotic normality is expected. Assuming this, the PF standard errors (the ones believed most trustworthy) suggest that all parameters are significantly non-zero at level 95%.

The findings suggest that the negative binomial distribution is preferred over the generalized Poisson, that the correlation in the series at lag one is negative, and that a BOGO event indeed increases sales.

Turning to residual diagnostics, the plots in Figure 7 are for the negative binomial-AR(3) fit and suggest that the model has captured both the marginal distribution and the dependence structure. The residuals here were computed using (71).

Parameters	ϕ_1	ϕ_2	ϕ_3	β_0	β_1	k
GL Estimates	-0.447	0.145	0.208	2.433	0.569	0.884
GL Standard Errors	0.175	0.171	0.130	0.095	0.115	0.207
PF Estimates	-0.341	0.223	0.291	2.264	1.01	1.21
PF Standard Errors	0.100	0.107	0.102	0.142	0.207	0.205

Table 2: Estimates and standard errors of the negative binomial-AR(3) model.

Parameters	ϕ_1	ϕ_2	ϕ_3	β_0	β_1	a
GL Estimates	-0.498	0.104	0.188	2.450	0.467	0.201
GL Standard Errors	0.245	0.250	0.161	0.095	0.108	0.036
PF Estimates	-0.331	0.178	0.232	2.211	1.038	0.298
PF Standard Errors	0.086	0.098	0.091	0.144	0.301	0.038

Table 3: Estimates and standard errors of the generalized Poisson-AR(3) model.

Finally, we assess the predictive ability of the two fits via the non-randomized histograms shown in Figure 8 and discussed in detailed in Section 3.4. We selected ten bins at the points $h/10, h = 1, \dots, 10$ as is typical in the literature. The negative binomial PIT plot suggests a satisfactory predictive ability with most bar heights being close to 0.1 (1 over the number of bins). In comparison, the generalized Poisson fit deviates more from the uniform distribution, with somewhat more pronounced peaks and valleys. We remind the reader here that PIT plots are known to be sensitive for smaller series lengths. Quantifying this uncertainty (for each bin) through a statistical test is well beyond the scope of this paper. Nevertheless, we gauged the variability of the uniform distribution's bin heights through a small experiment. Specifically, 500 synthetic realizations of sample size $T = 104$ were generated and the percentiles of all bin heights were collected. The 5th and 95th percentiles ranged in the intervals $(0.048, 0.058)$ and $(0.145, 0.154)$ respectively, suggesting that the peaks and valleys of the negative binomial PIT plot (which are within these percentiles) are mild; that is, uniformity is plausible.

6 Conclusions and comments

This paper developed the theory and methods for a Gaussian copula-based stationary count time series model. By using a Gaussian copula and Hermite expansions, a very general model class was devised. In particular, the autocorrelations in the series can be positive or negative, and in a pairwise sense, span the range of all achievable correlations. The series can have any marginal distribution desired, thereby improving classical DARMA and INARMA count time series methods. On inferential levels, autocovariances of the model were computed via Hermite expansions, allowing for Gaussian pseudo-likelihood and implied Yule-Walker inference procedures. A particle filtering HMM approach was also developed and produced approximate likelihood estimators that were demonstrated to be more accurate than Gaussian pseudo-likelihood and implied Yule-Walker estimators in some cases. These results complement the importance sampling methods for copula likelihoods in [47]. The methods were used in a simulation study and were applied in a regression analysis of a count

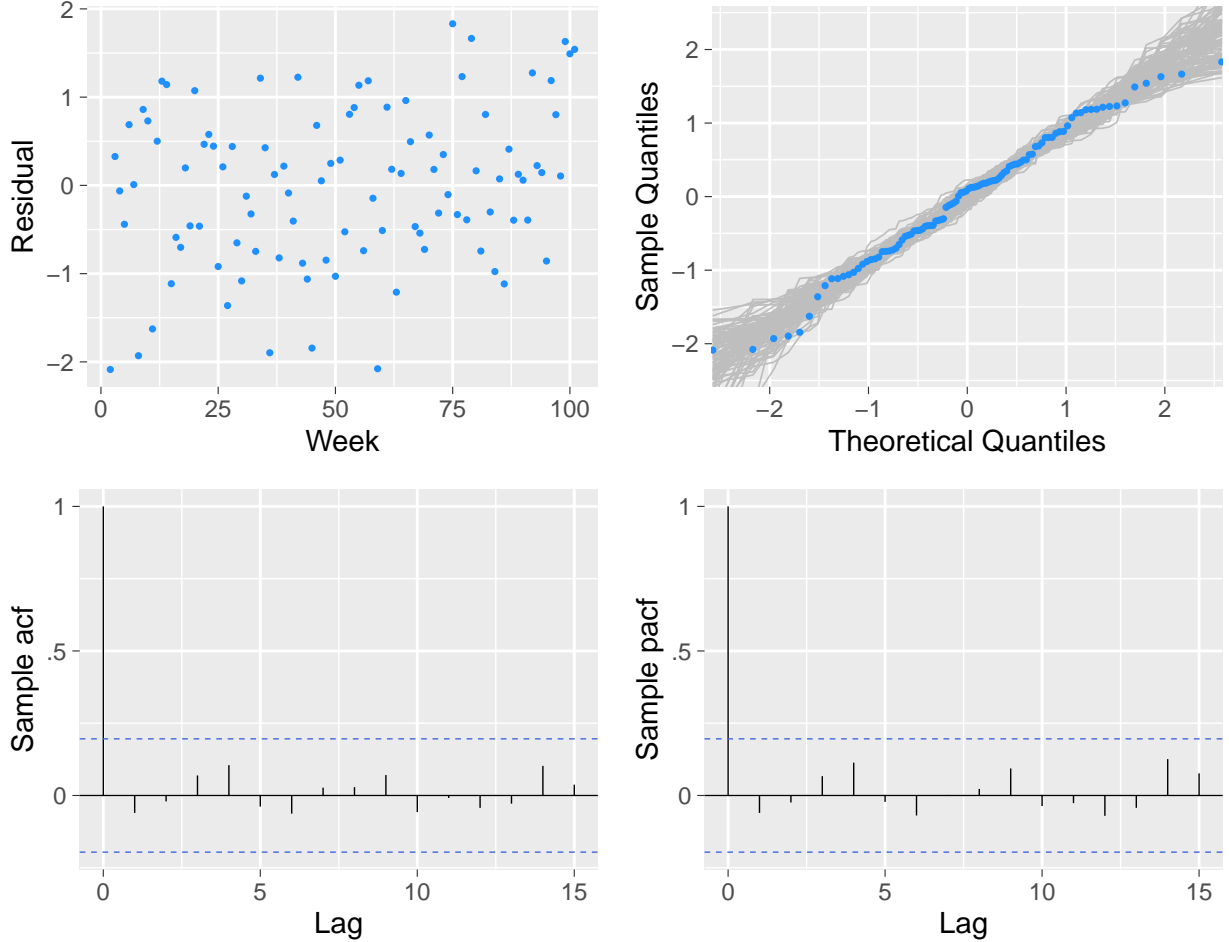


Figure 7: The upper left plot displays the estimated residuals against time. The upper right plot is a QQ plot for normality of the estimated residuals. The gray lines in the QQ plot are 100 realizations from a normal distribution with size, mean and standard deviation matching the residual sample counterparts. The two plots on the bottom display the sample autocorrelations and partial autocorrelations of the estimated residuals.

series of weekly sales from a large grocery chain. This series of small counts had a “buy one get one free” covariate, overdispersion, and negative lag one correlation. Model fits and predictive abilities of the methods were illustrated with generalized Poisson and negative binomial marginal distributions.

While the paper provides a reasonably complete treatment for copula count time series models, avenues for future research remain. First, some statistical issues — asymptotic normality of parameter estimators is one example — were not addressed here. Second, the paper only considers univariate methods. Multivariate count time series models akin to those in [48] could be developed by switching $\{Z_t\}$ to a multivariate Gaussian process $\{\mathbf{Z}_t\}$, where the components of \mathbf{Z}_t are correlated for each fixed t , but each have a standard normal marginal distribution. The details for such a construction would proceed akin to the methods developed here. Third, while the count case is considered here, the same methods will also

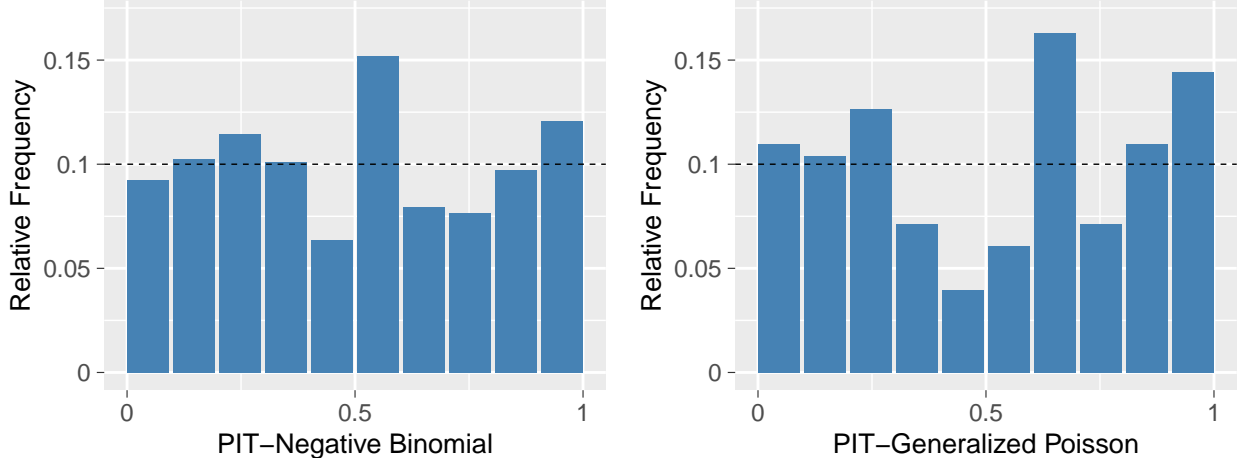


Figure 8: PIT residual histograms for the estimated models in Tables 2 and 3.

produce stationary time series having any general prescribed continuous distribution. In fact, in the continuous case, the change of variables density formula yields an exact likelihood for the model; this tactic was recently pursued in [52] for extreme value modeling. Finally, the same methods should prove useful in constructing spatial and spatio-temporal processes having any prescribed marginal distribution. While [15, 25] recently addressed this issue in the spatial setting, additional work is needed, including exploring spatial Markov properties of the model and likelihood evaluation techniques. To the best of our knowledge, no copula-based work has been conducted for space-time count modeling to date.

A Proofs

This section proves some of our results, beginning with Proposition 2.1.

Proof of Proposition 2.1: We first derive the expression (30) informally and then furnish the technicalities. When $G(\cdot)$ in (1) and (2) is continuous and differentiable, the derivative of the link function can be obtained from the Price Theorem (Theorem 5.8.5 in [46]); namely, for $u \in (-1, 1)$,

$$L'(u) = \frac{1}{\gamma_X(0)} \mathbb{E}[G'(Z_0)G'(Z_1)] \Big|_{\text{Corr}(Z_0, Z_1)=u} \quad (75)$$

(the notation indicates that the correlation between the standard Gaussian pair (Z_0, Z_1) is u). If G is further nondecreasing, then $G'(x) \geq 0$ for all x and (75) implies that $L'(u) \geq 0$ for all u . This is the argument in [23]. While our G is nondecreasing, it can be seen to be piecewise constant via (19) and is hence not differentiable at its jump points.

To remedy this, we approximate G by differentiable functions, apply (75), and take limits

in the approximation error. Executing on this, for $\epsilon > 0$ and $U \stackrel{\mathcal{D}}{=} \mathcal{N}(0, 1)$, set

$$\begin{aligned}
G_\epsilon(x) &= \mathbb{E}[G(x + \epsilon U)] = \int_{-\infty}^{\infty} G(z) \frac{e^{-\frac{(x-z)^2}{2\epsilon^2}}}{\sqrt{2\pi\epsilon}} dz \\
&= \sum_{n=0}^{\infty} n \int_{\Phi^{-1}(C_{n-1})}^{\Phi^{-1}(C_n)} \frac{e^{-\frac{(x-z)^2}{2\epsilon^2}}}{\sqrt{2\pi\epsilon}} dz \\
&= \sum_{n=0}^{\infty} n \int_{\Phi^{-1}(C_{n-1})-x}^{\Phi^{-1}(C_n)-x} \frac{e^{-\frac{w^2}{2\epsilon^2}}}{\sqrt{2\pi\epsilon}} dw,
\end{aligned} \tag{76}$$

where the expression in (19) was substituted for $G(z)$. As $\epsilon \downarrow 0$, $G_\epsilon(x)$ approximates $G(x)$ since the ‘‘kernel’’ $e^{-\frac{(x-z)^2}{2\epsilon^2}}/(\sqrt{2\pi\epsilon})$ acts like Dirac’s delta function $\delta_{\{x\}}(z)$ at $z = x$. Let L_ϵ be the link function induced by G_ϵ , and $X_t^{(\epsilon)} = G_\epsilon(Z_t)$ its corresponding time series. Observe that $G_\epsilon(x)$ is nondecreasing and is differentiable by (76) with derivative

$$G'_\epsilon(x) = \frac{1}{\sqrt{2\pi\epsilon}} \sum_{n=0}^{\infty} n \left[e^{-\frac{(\Phi^{-1}(C_{n-1})-x)^2}{2\epsilon^2}} - e^{-\frac{(\Phi^{-1}(C_n)-x)^2}{2\epsilon^2}} \right] = \frac{1}{\sqrt{2\pi\epsilon}} \sum_{n=0}^{\infty} e^{-\frac{(\Phi^{-1}(C_n)-x)^2}{2\epsilon^2}}, \tag{77}$$

where the last step uses the telescoping nature of the series, justifiable from the finiteness of $\mathbb{E}[X_t^p]$ for some $p > 1$ analogously to (20) and (21). Formula (75) now yields

$$\begin{aligned}
L'_\epsilon(u) &= \frac{1}{\gamma_{X^{(\epsilon)}}(0)} \mathbb{E}[G'_\epsilon(Z_0)G'_\epsilon(Z_1)] \Big|_{\text{Corr}(Z_0, Z_1)=u} \\
&= \frac{1}{\gamma_{X^{(\epsilon)}}(0)} \int_{-\infty}^{\infty} \int_{-\infty}^{\infty} G'_\epsilon(z_0)G'_\epsilon(z_1) \frac{1}{2\pi\sqrt{1-u^2}} e^{-\frac{1}{2(1-u^2)}(z_0^2+z_1^2-2uz_0z_1)} dz_0 dz_1 \\
&= \frac{1}{\gamma_{X^{(\epsilon)}}(0)} \sum_{n_0=0}^{\infty} \sum_{n_1=0}^{\infty} \int_{-\infty}^{\infty} \int_{-\infty}^{\infty} \frac{1}{\sqrt{2\pi\epsilon}} e^{-\frac{(\Phi^{-1}(C_{n_0})-z_0)^2}{2\epsilon^2}} \frac{1}{\sqrt{2\pi\epsilon}} e^{-\frac{(\Phi^{-1}(C_{n_1})-z_1)^2}{2\epsilon^2}} \times \\
&\quad \times \frac{1}{2\pi\sqrt{1-u^2}} e^{-\frac{1}{2(1-u^2)}(z_0^2+z_1^2-2uz_0z_1)} dz_0 dz_1.
\end{aligned} \tag{78}$$

Noting again that $e^{-\frac{(x-z)^2}{2\epsilon^2}}/(\sqrt{2\pi\epsilon})$ acts like a Dirac’s delta function $\delta_{\{x\}}(z)$, the limit as $\epsilon \downarrow 0$ should be

$$L'(u) = \frac{1}{\gamma_X(0)} \sum_{n_0=0}^{\infty} \sum_{n_1=0}^{\infty} \frac{1}{2\pi\sqrt{1-u^2}} e^{-\frac{1}{2(1-u^2)}(\Phi^{-1}(C_{n_0})^2+\Phi^{-1}(C_{n_1})^2-2u\Phi^{-1}(C_{n_0})\Phi^{-1}(C_{n_1}))}, \tag{79}$$

which is (30) and is always non-negative. Note that the derivative of L always exists in $u \in (-1, 1)$ since $L(u)$ is a power series with positive coefficients that sum to unity.

The formal justification of (79) proceeds as follows. We focus only on proving that $L'_\epsilon(u)$ converges to $L'(u)$, which is the most difficult step. For this, we first need an expression for the Hermite coefficients of $G_\epsilon(\cdot)$, denoted by $g_{\epsilon,k}$. These will be compared to the Hermite

coefficients g_k of G . Using $H_k(x + y) = \sum_{\ell=0}^k \binom{k}{\ell} y^{k-\ell} H_\ell(x)$, note that

$$\begin{aligned} G_\epsilon(z) &= \mathbb{E}[G(x + \epsilon U)] = \mathbb{E} \left[\sum_{k=0}^{\infty} g_k H_k(x + \epsilon U) \right] \\ &= \mathbb{E} \left[\sum_{k=0}^{\infty} g_k \sum_{\ell=0}^k \binom{k}{\ell} (\epsilon U)^{k-\ell} H_\ell(x) \right] \\ &= \sum_{\ell=0}^{\infty} H_\ell(x) \sum_{k=\ell}^{\infty} g_k \epsilon^{k-\ell} \binom{k}{\ell} \mathbb{E}[U^{k-\ell}]. \end{aligned}$$

Then, after changing summation indices and using that $\mathbb{E}[U^p] = 0$ if p is odd, and equal to $(p-1)!!$ if p is even, where $k!! = 1 \times 3 \times \dots \times k$ when k is odd, we get

$$g_{\epsilon,k} = g_k + \sum_{q=1}^{\infty} g_{k+2q} \epsilon^{2q} \binom{k+2q}{k} (2q-1)!! = g_k + \sum_{q=1}^{\infty} g_{k+2q} \epsilon^{2q} \frac{(k+2q)!}{k! 2^q q!}. \quad (80)$$

This implies that

$$|g_k^2 - g_{k,\epsilon}^2| \leq 2|g_k| \sum_{q=1}^{\infty} |g_{k+2q}| \epsilon^{2q} \frac{(k+2q)!}{k! 2^q q!} + \left(\sum_{q=1}^{\infty} |g_{k+2q}| \epsilon^{2q} \frac{(k+2q)!}{k! 2^q q!} \right)^2. \quad (81)$$

The Cauchy-Schwarz inequality gives the bound

$$\begin{aligned} \sum_{q=1}^{\infty} |g_{k+2q}| \epsilon^{2q} \frac{(k+2q)!}{k! 2^q q!} &\leq \left(\sum_{q=1}^{\infty} g_{k+2q}^2 (k+2q)! \right)^{1/2} \left(\sum_{q=1}^{\infty} \epsilon^{4q} \frac{(k+2q)!}{(k!)^2 (2^q q!)^2} \right)^{1/2} \\ &\leq \frac{M_k}{(k!)^{1/2}} \left(\sum_{q=1}^{\infty} \epsilon^{4q} \frac{(k+2q)!}{k! (2q)!} \right)^{1/2}, \end{aligned}$$

where M_k is some finite constant that converges to zero as $k \rightarrow \infty$. Here, we have used that $\sum_{q=1}^{\infty} g_{k+2q}^2 (k+2q)! \rightarrow 0$ as $k \rightarrow \infty$, which is justifiable via (11), and the fact that $(2^q q!)^2$ is of the same order as $(2q)!!$.

To bound sums of form $\sum_{p=1}^{\infty} \epsilon^{2p} \binom{k+p}{p}$, use $\sum_{p=0}^{\infty} x^p \binom{k+p}{p} = (1-x)^{-k-1}$, $|x| < 1$. Collecting the above bounds and returning to (81) gives

$$|g_k^2 - g_{k,\epsilon}^2| \leq \frac{2M_k |g_k|}{(k!)^{1/2}} \left[(1 - \epsilon^2)^{-k-1} - 1 \right]^{1/2} + \frac{M_k^2}{k!} [(1 - \epsilon^2)^{-k-1} - 1]. \quad (82)$$

The rest of the argument is straightforward with this bound; in particular, note from (13) that

$$L'(u) = \sum_{k=1}^{\infty} \frac{g_k^2 k!}{\gamma_X(0)} k u^{k-1},$$

where the series converges for $u \in (-1, 1)$ since the “extra” k gets dominated by u^{k-1} . Similarly,

$$L'_\epsilon(u) = \sum_{k=1}^{\infty} \frac{g_{\epsilon,k}^2 k!}{\gamma_{X^{(\epsilon)}}(0)} k u^{k-1}.$$

Then,

$$|L'(u) - L'_\epsilon(u)| \leq \left| \frac{1}{\gamma_X(0)} - \frac{1}{\gamma_{X^{(\epsilon)}}(0)} \right| \sum_{k=1}^{\infty} g_k^2 k! k |u|^{k-1} + \frac{1}{\gamma_{X^{(\epsilon)}}(0)} \sum_{k=1}^{\infty} |g_k^2 - g_{\epsilon,k}^2| k! k |u|^{k-1}. \quad (83)$$

For example, the series in the last bound converges to 0 as $\epsilon \downarrow 0$. Indeed, by using (82), this follows if

$$\sum_{k=1}^{\infty} |g_k|(k!)^{1/2} [(1 - \epsilon^2)^{-k-1} - 1]^{1/2} k |u|^{k-1} \rightarrow 0, \quad \sum_{k=1}^{\infty} [(1 - \epsilon^2)^{-k-1} - 1] k |u|^{k-1} \rightarrow 0.$$

In both of these cases, the convergence follows from the dominated convergence theorem since $(1 - \epsilon^2)^{-k-1} - 1 \rightarrow 0$ as $\epsilon \downarrow 0$. By using (11), one can similarly show that $\gamma_{X^{(\epsilon)}}(0) \rightarrow \gamma_X(0)$. Hence, we conclude that $L'_\epsilon(u) \rightarrow L'(u)$ as $\epsilon \rightarrow 0$. \square

Lemma 2.2 will follow from the following more general result.

Lemma A.1. *For bounded functions h_1 and h_2 ,*

$$\mathbb{E}_{\mathcal{H}_t}[h_1(Z_0, \dots, Z_t)] = \frac{\int_{\{z_s \in A_{x_s, s=0, \dots, t}\}} h_1(z_0, \dots, z_t) e^{-\frac{1}{2} \sum_{s=0}^t (z_s - \hat{z}_s)^2 / r_s^2} dz_0 \dots dz_t}{\int_{\{z_s \in A_{x_s, s=0, \dots, t}\}} e^{-\frac{1}{2} \sum_{s=0}^t (z_s - \hat{z}_s)^2 / r_s^2} dz_0 \dots dz_t} \quad (84)$$

and

$$\mathbb{E}_{\mathcal{H}_t}[h_2(Z_0, \dots, Z_{t+1})] = \frac{\int_{\mathbb{R}} \int_{\{z_s \in A_{x_s, s=0, \dots, t}\}} h_2(z_0, \dots, z_{t+1}) e^{-\frac{1}{2} \sum_{s=0}^{t+1} (z_s - \hat{z}_s)^2 / r_s^2} dz_0 \dots dz_t dz_{t+1}}{\int_{\mathbb{R}} \int_{\{z_s \in A_{x_s, s=0, \dots, t}\}} e^{-\frac{1}{2} \sum_{s=0}^{t+1} (z_s - \hat{z}_s)^2 / r_s^2} dz_0 \dots dz_{t+1}}, \quad (85)$$

where $\mathbb{E}_{\mathcal{H}_t}$ refers to an expectation conditioned on the history $\mathcal{H}_t = \{X_0 = x_0, \dots, X_t = x_t\}$. Moreover, for bounded functions h_3 ,

$$\mathbb{E}[h_3(X_0, \dots, X_t)] = \int_{\mathbb{R}^{t+1}} h_3(G(z_0), \dots, G(z_t)) \frac{e^{-\frac{1}{2} \sum_{s=0}^t (z_s - \hat{z}_s)^2 / r_s^2}}{(2\pi)^{(t+1)/2} r_0 \dots r_t} dz_0 \dots dz_t. \quad (86)$$

Proof: The Innovations form of the joint Gaussian density (see Section 8.6 of [6]) gives

$$\mathbb{E}[h(Z_0, \dots, Z_t)] = \int_{\mathbb{R}^{t+1}} h(z_0, \dots, z_t) \frac{e^{-\frac{1}{2} \sum_{s=0}^t (z_s - \hat{z}_s)^2 / r_s^2}}{(2\pi)^{(t+1)/2} r_0 \dots r_t} dz_0 \dots dz_t. \quad (87)$$

To obtain (84), note that by (32) for a bounded function g we have,

$$\mathbb{E}[g(X_0, \dots, X_t) h_1(Z_0, \dots, Z_t)] = \mathbb{E}[g(G(Z_0), \dots, G(Z_t)) h_1(Z_0, \dots, Z_t)]$$

$$\begin{aligned}
&= \sum_{i_0, \dots, i_t \in \mathbb{N}_0} \mathbb{E}[g(G(Z_0), \dots, G(Z_t)) h_1(Z_0, \dots, Z_t) 1_{\{G(Z_s)=i_s, s=0, \dots, t\}}] \\
&= \sum_{i_0, \dots, i_t \in \mathbb{N}_0} g(i_0, \dots, i_t) \mathbb{E}[h_1(Z_0, \dots, Z_t) 1_{\{Z_s \in A_{i_s}, s=0, \dots, t\}}] \\
&= \sum_{i_0, \dots, i_t \in \mathbb{N}_0} g(i_0, \dots, i_t) \frac{\mathbb{E}[h_1(Z_0, \dots, Z_t) 1_{\{Z_s \in A_{i_s}, s=0, \dots, t\}}]}{\mathbb{E}[1_{\{Z_s \in A_{i_s}, s=0, \dots, t\}}]} \mathbb{P}(X_s = i_s, s = 0, \dots, t),
\end{aligned}$$

implying that

$$\mathbb{E}_{\mathcal{H}_t}[h_1(Z_0, \dots, Z_t)] = \frac{\mathbb{E}[h_1(Z_0, \dots, Z_t) 1_{\{Z_s \in A_{x_s}, s=0, \dots, t\}}]}{\mathbb{E}[1_{\{Z_s \in A_{x_s}, s=0, \dots, t\}}]},$$

which can be expressed as in (84) by invoking (87). The relation (85) is similarly proven. Equation (86) follows from (87) since $h_3(X_0, \dots, X_t) = h_3(G(Z_0), \dots, G(Z_t))$. \square

Remark A.1. The relation (86) implies, in particular, that

$$\mathbb{P}(X_0 = x_0, \dots, X_t = x_t) = \int_{\{Z_s \in A_{x_s}, s=0, \dots, t\}} \frac{e^{-\frac{1}{2} \sum_{s=0}^t (z_s - \hat{z}_s)^2 / r_s^2}}{(2\pi)^{(t+1)/2} r_0 \dots r_t} dz_0 \dots dz_t. \quad (88)$$

We next prove Lemma 2.2 .

Proof of Lemma 2.2: The relation (33) follows from (84) since $\hat{Z}_{t+1} = \hat{Z}_{t+1}(Z_0, \dots, Z_t)$, the notation indicating dependence of \hat{Z}_{t+1} on Z_0, \dots, Z_t . Similarly, (34) follows from (85) since $V(X_{t+1}) = V(G(Z_{t+1}))$. \square

Finally, we prove Proposition 2.2.

Proof of Proposition 2.2: The superscript i is suppressed for notational simplicity. Note that

$$\begin{aligned}
\mathbb{E}_{\mathcal{H}_t} \left[w_t V(\hat{Z}_{t+1}) \right] &= \mathbb{E}_{\mathcal{H}_t} \left[w_{t-1} w_t(\hat{Z}_t) V(\hat{z}_{t+1}(Z_0, \dots, Z_t)) \right] \\
&= \mathbb{E}_{\mathcal{H}_t} \left[w_{t-1} w_t(\hat{Z}_t) V(\hat{z}_{t+1}(Z_0, \dots, \hat{Z}_t + r_t \epsilon_t)) \right] \\
&= \mathbb{E}_{\mathcal{H}_t} \left[\mathbb{E}_{\mathcal{H}_t} [w_{t-1} w_t(\hat{Z}_t) V(\hat{z}_{t+1}(Z_0, \dots, \hat{Z}_t + r_t \epsilon_t)) | Z_0, \dots, Z_{t-1}] \right] \\
&= \mathbb{E}_{\mathcal{H}_t} \left[w_{t-1} w_t(\hat{Z}_t) \frac{\int_{A_{x_t}} V(\hat{z}_{t+1}(Z_0, \dots, Z_{t-1}, z_t)) \frac{e^{-\frac{1}{2r_t}(z_t - \hat{Z}_t)^2}}{\sqrt{2\pi r_t^2}} dz_t}{\int_{A_{x_t}} \frac{e^{-\frac{1}{2r_t}(z_t - \hat{Z}_t)^2}}{\sqrt{2\pi r_t^2}} dz_t} \right] \\
&= \mathbb{E}_{\mathcal{H}_t} \left[w_{t-1} \int_{A_{x_t}} V(\hat{z}_{t+1}(Z_0, \dots, Z_{t-1}, z_t)) \frac{e^{-\frac{1}{2r_t}(z_t - \hat{Z}_t)^2}}{\sqrt{2\pi r_t^2}} dz_t \right],
\end{aligned}$$

where the definitions of ϵ_t in Step 2 of the SIS algorithm and $w_t(z)$ as in (43) have been used. A similar argument leads to

$$\mathbb{E}_{\mathcal{H}_t} \left[w_{t-2} \int_{A_{x_{t-1}}} \int_{A_{x_t}} V(\hat{z}_{t+1}(Z_0, \dots, Z_{t-2}, z_{t-1}, z_t)) \frac{e^{-\frac{1}{2r_{t-1}}(z_{t-1} - \hat{Z}_{t-1})^2 - \frac{1}{2r_t}(z_t - \hat{z}_t(Z_0, \dots, z_{t-1}))^2}}{\sqrt{2\pi r_{t-1}^2} \sqrt{2\pi r_t^2}} dz_{t-1} dz_t \right].$$

Further similar iterations yield

$$\mathbb{E}_{\mathcal{H}_t}[w_t V(\hat{Z}_{t+1})] = \frac{\int_{z_s \in A_{x_s}, s=0, \dots, t} V(\hat{z}_{t+1}) \frac{e^{-\frac{1}{2} \sum_{s=0}^t (z_s - \hat{z}_s)^2 / r_s^2}}{(2\pi)^{(t+1)/2} r_0 \dots r_t} dz_0 \dots dz_t}{\int_{z_0 \in A_{x_0}} \frac{e^{-z_0^2/2}}{(2\pi)^{1/2} r_0} dz_0}$$

(the term in the denominator does not cancel out since $w_0 = 1$), and the proposition now follows via (33). \square

Acknowledgments. The authors thank the referees and Associate Editors for comments that helped improve this manuscript.

References

- [1] D. Ardia, K. M. Mullen, B. G. Peterson, and J. Ulrich. *DEoptim: Differential Evolution in R*, 2016. Version 2.2-4.
- [2] S. Asmussen. Modeling and performance of bonus-malus systems: stationarity versus age-correction. *Risks*, 2:49–73, 2014.
- [3] M. Belyaev, E. Burnaev, and Y. Kapushev. Gaussian process regression for structured data sets. In A. Gammerman, V. Vovk, and H. Papadopoulos, editors, *Statistical Learning and Data Sciences: Third International Symposium, SLDS 2015, Egham, UK, April 20-23, 2015, Proceedings*. Springer International Publishing, Switzerland, 2015.
- [4] M. A. Benjamin, R. A. Rigby, and D. M. Stasinopoulos. Generalized autoregressive moving average models. *Journal of the American Statistical Association*, 98(461):214–223, 2003.
- [5] P. A. Blight. Time series formed from the superposition of discrete renewal processes. *Journal of Applied Probability*, 26:189–195, 1989.
- [6] P. J. Brockwell and R. A. Davis. *Time Series: Theory and Methods*. Springer-Verlag, New York, second edition, 1991.
- [7] M. C. Cario and B. L. Nelson. Modeling and generating random vectors with arbitrary marginal distributions and correlation matrix. *Technical Report*, Department of Industrial Engineering and Management Sciences, Northwestern University, 1997.
- [8] H. Chen. Initialization of NORTA: Generation of random vectors with specified marginals and correlations. *Inform Journal on Computing*, 13:312–331, 2001.
- [9] X. Chen and Y. Fang. Estimation of copula-based semiparametric time series models. *Journal of Econometrics*, 130:307–335, 2006.
- [10] Y. Cui and R. B. Lund. A new look at time series of counts. *Biometrika*, 96:781–792, 2009.

- [11] C. Czado, T. Gneiting, and L. Held. Predictive model assessment for count data. *Biometrics*, 65:1254–1261, 2009.
- [12] R. A. Davis, W. T. M. Dunsmuir, and S. B. Streett. Observation-driven models for Poisson counts. *Biometrika*, 90:777–790, 2003.
- [13] R. A. Davis, W. T. M. Dunsmuir, and Y. Wang. Modeling time series of count data. In: *Asymptotics, Nonparametrics, and Time Series. Statistical Textbooks and Monographs*, 158:63–114, 1999.
- [14] R. A. Davis, S. H. Holan, R. B. Lund, and N. Ravishanker, editors. *Handbook of Discrete-Valued Time Series*. CRC Press, Boca Raton, Florida, USA, 2016.
- [15] V. De Oliveira. Hierarchical Poisson models for spatial count data. *Journal of Multivariate Analysis*, 122:393–408, 2016.
- [16] R. Douc, E. Moulines, and D. S. Stoffer. *Nonlinear Time Series: Theory, Methods, and Applications with R Examples*. Chapman & Hall/CRC Texts in Statistical Science Series. Chapman & Hall/CRC Press, Boca Raton, FL, 2014.
- [17] F. Famoye. Restricted generalized Poisson regression model. *Communications in Statistics-Theory and Methods*, 22(5):1335–1354, 1993.
- [18] K. Fokianos. Some recent progress in count time series. *Statistics*, 45:49–58, 2011.
- [19] K. Fokianos and B. Kedem. Prediction and classification of non-stationary categorical time series. *Journal of Multivariate Analysis*, 67:277–296, 1998.
- [20] K. Fokianos and B. Kedem. Regression theory for categorical time series. *Statistical Science*, 18:357–376, 2003.
- [21] D. Freedman. On the so-called “Huber sandwich estimator” and “robust standard errors”. *The American Statistician*, 60:299–302, 2006.
- [22] A. Genz. Numerical computation of rectangular bivariate and trivariate normal and t probabilities. *Statistics and Computing*, 14(3):251–260, 2004.
- [23] M. Grigoriu. Multivariate distributions with specified marginals: applications to wind engineering. *Journal of Engineering Mechanics*, 133:174–184, 2007.
- [24] V. A. Hajivassiliou and P. A. Ruud. Classical estimation methods for LDV models using simulation. In *Handbook of Econometrics, Vol. IV*, volume 2 of *Handbooks in Econometrics*, pages 2383–2441. North-Holland, Amsterdam, 1994.
- [25] Z. Han and V. De Oliveira. On the correlation structure of Gaussian copula models for geostatistical count data. *Australian & New Zealand Journal of Statistics*, 58:47–69, 2016.
- [26] Z. Han and V. De Oliveira. gcKrig: A R package for the analysis of geostatistical count data using Gaussian copulas. *Journal of Statistical Software*, 87(1):1–32, 2018.

- [27] Z. Han and V. De Oliveira. Maximum likelihood estimation of Gaussian copula models for geostatistical count data. *Communications in Statistics-Simulation and Computation*, pages 1–25, 2018.
- [28] P. Henrici. *Applied and Computational Complex Analysis, Volume 1: Power Series, Integration, Conformal Mapping, Location of Zero*, volume 4. John Wiley & Sons, 1988.
- [29] P. A. Jacobs and P. A. W. Lewis. Discrete time series generated by mixtures I: Correlational and runs properties. *Journal of the Royal Statistical Society*, 40:94–105, 1978a.
- [30] P. A. Jacobs and P. A. W. Lewis. Discrete time series generated by mixtures II: Asymptotic properties. *Journal of the Royal Statistical Society*, 40:222–228, 1978b.
- [31] Yisu Jia, Robert Lund, and James Livsey. Superpositioned stationary count time series. *Probability in the Engineering and Informational Sciences*, pages 1–19, 2016.
- [32] H. Joe. Time series models with univariate margins in the convolution-closed infinitely divisible class. *Journal of Applied Probability*, 33:664–677, 1996.
- [33] H. Joe and R. Zhu. Generalized Poisson distribution: the property of mixture of Poisson and comparison with negative binomial distribution. *Biometrical Journal: Journal of Mathematical Methods in Biosciences*, 47(2):219–229, 2005.
- [34] M. Kachour and J. F. Yao. First order rounded integer valued autoregressive (RINAR(1)) processes. *Journal of Time Series Analysis*, 30:417–448, 2009.
- [35] S. Kolassa. Evaluating predictive count data distributions in retail sales forecasting. *International Journal of Forecasting*, 32:788–803, 2016.
- [36] H. Lennon. *Gaussian copula modelling for integer-valued time series*. PhD thesis, The University of Manchester, 2016.
- [37] J. Livsey, R. B. Lund, S. Kechagias, and V. Pipiras. Multivariate integer-valued time series with flexible autocovariances and their application to major hurricane counts. *Annals of Applied Statistics*, 12:408–431, 2018.
- [38] R. B. Lund and J. Livsey. Renewal-based count time series. In R. A. Davis, S. H. Holan, R. B. Lund, and N. Ravishanker, editors, *Handbook of Discrete-Valued Time Series*. CRC Press, New York City, NY, 2015.
- [39] G. Masarotto and C. Varin. Gaussian copula marginal regression. *Electronic Journal of Statistics*, 6:1517–1549, 2012.
- [40] G. Masarotto and C. Varin. Gaussian copula regression in R. *Journal of Statistical Software*, 77:1–26, 2017.
- [41] E. McKenzie. Some simple models for discrete variate time series. *Water Resources Bulletin*, 21:645–650, 1985.

- [42] E. McKenzie. Autoregressive-moving average processes with negative-binomial and geometric marginal distributions. *Advances in Applied Probability*, 18:679–705, 1986.
- [43] E. McKenzie. Some ARMA models for dependent sequences of Poisson counts. *Advances in Applied Probability*, 20:822–835, 1988.
- [44] K. Mullen, D. Ardia, D. Gil, D. Windover, and J. Cline. DEoptim: An R package for global optimization by differential evolution. *Journal of Statistical Software*, 40(6):1–26, 2011.
- [45] A. K. Nikoloulopoulos and D. Karlis. On modeling count data: a comparison of some well-known discrete distributions. *Journal of Statistical Computation and Simulation*, 78(3):437–457, 2008.
- [46] V. Pipiras and M. S. Taqqu. *Long-Range Dependence and Self-Similarity*, volume 45. Cambridge University Press, 2017.
- [47] M. S. Smith and M. A. Khaled. Estimation of copula models with discrete margins via Bayesian data augmentation. *Journal of the American Statistical Association*, 107:290–303, 2012.
- [48] P. Song, M. Li, and P. Zhang. Vector generalized linear models: a Gaussian copula approach. In P. Jaworski, F. Durante, and W.K. Härdle, editors, *Copulae in Mathematical and Quantitative Finance*. Springer, Heidelberg, Germany, 2013.
- [49] R. Storn and K. Price. Differential evolution—a simple and efficient heuristic for global optimization over continuous spaces. *Journal of Global Optimization*, 11(4):341–359, 1997.
- [50] Y. L. Tong. *The Multivariate Normal Distribution*. Springer-Verlag, New York City, 1990.
- [51] W. Whitt. Bivariate distributions with given marginals. *The Annals of Statistics*, 4(6):1280–1289, 1976.
- [52] L. Zhu, X. Liu, and R. B. Lund. A likelihood for correlated extreme series. *Environmetrics*, 30(4):e2546, 2019.